NAVAL POSTGRADUATE SCHOOL
Monterey, California

THESIS

POSITIONING OF JAMMING AIRCRAFT
USING THE INTEGRATED REFRACTIVE EFFECTS
PREDICTION SYSTEM

by

Thomas W. White

October 1982

Thesis Advisor: G. E. Schacher

Approved for public release; distribution unlimited.

REPORT DOCUMENTATION PAGE		READ INSTRUCTIONS BEFORE COMPLETING FORM
1. REPORT NUMBER	2. GOVT ACCESSION NO.	3. RECIPIENT'S CATALOG NUMBER
4. TITLE (and Subtitle) Positioning of Jamming Aircraft Using the Integrated Refractive Effects Prediction System		5. TYPE OF REPORT & PERIOD COVERED Master's Thesis; October 1982 6. PERFORMING ORG. REPORT NUMBER
7. AUTHOR(s) Thomas W. White		8. CONTRACT OR GRANT NUMBER(s)
9. PERFORMING ORGANIZATION NAME AND ADDRESS Naval Postgraduate School Monterey, California 93940		10. PROGRAM ELEMENT, PROJECT, TASK AREA & WORK UNIT NUMBERS
11. CONTROLLING OFFICE NAME AND ADDRESS Naval Postgraduate School Monterey, California 93940		12. REPORT DATE October 1982 13. NUMBER OF PAGES 114
14. MONITORING AGENCY NAME & ADDRESS(if different from Controlling Office)		15. SECURITY CLASS. (of this report) Unclassified 15a. DECLASSIFICATION/DOWNGRADING SCHEDULE

16. DISTRIBUTION STATEMENT (of this Report)

Approved for public release; distribution unlimited.

17. DISTRIBUTION STATEMENT (of the abstract entered in Block 20, if different from Report)

18. SUPPLEMENTARY NOTES

19. KEY WORDS (Continue on reverse side if necessary and identify by block number)
Anomalous Propagation, IREPS (Integrated Refractive Effects Prediction System), Electromagnetic Propagation, Ducting, Tactical Electronic Warfare, Self-protection Jamming, Standoff Jamming

20. ABSTRACT (Continue on reverse side if necessary and identify by block number)

Tactical ECM planning has historically considered only horizontal positioning of self-protection and standoff jamming systems. Failure to consider vertical positioning of the jammer, and how the environment affects that positioning, can lead to substantially reduced jamming effectiveness. The effects of radar and jamming system antenna patterns and environmental considerations are discussed. The Integrated

#20 - ABSTRACT - (CONTINUED)

Refractive Effects Prediction System (IREPS) incorporates these effects, but not in a form that is convenient for ECM planning. However, as it is now configured, IREPS can be a useful tool. A step-by-step approach for using IREPS and the jamming equations to assist the ECM planner is given. Sample calculations for self-protection and standoff jamming under actual environmental conditions are provided.

Approved for public release; distribution unlimited.

Positioning of Jamming Aircraft Using the Integrated Refractive Effects Prediction System

by

Thomas W. White
Captain, United States Air Force
B.S., New Mexico State University, 1971

Submitted in partial fulfillment of the
requirements for the degree of

MASTER OF SCIENCE IN SYSTEMS TECHNOLOGY

from the

NAVAL POSTGRADUATE SCHOOL

October 1982

ABSTRACT

Tactical ECM planning has historically considered only horizontal positioning of self-protection and standoff jamming systems. Failure to consider vertical positioning of the jammer, and how the environment affects that positioning, can lead to substantially reduced jamming effectiveness. The effects of radar and jamming system antenna patterns and environmental considerations are discussed. The Integrated Refractive Effects Prediction System (IREPS) incorporates these effects, but not in a form that is convenient for ECM planning. However, as it is now configured, IREPS can be a useful tool. A step-by-step approach for using IREPS and the jamming equations to assist the ECM planner is given. Sample calculations for self-protection and standoff jamming under actual environmental conditions are provided.

TABLE OF CONTENTS

LIST OF TABLES

LIST OF FIGURES

ACKNOWLEDGMENTS

I wish to express my appreciation to Dr. Gordon Schacher for his guidance and assistance in preparing this thesis.

Special thanks go to Professor John Bouldry and Professor Ken Davidson for their encouragement in pursuing this thesis.

My appreciation is also extended to Mr. Herb Hitney and Mr. Claude Hattan at Naval Ocean Systems for their assistance in modifying the IREPS program for the jamming application.

I would like to thank my family, Beverly, Jamie and Jason for their patient and understanding during my studies at the Naval Postgraduate School.

I. INTRODUCTION

Electronic Warfare (EW) refers to that broad range of modern warfare that utilizes radiated electromagnetic energy. In general, the purpose is to utilize electromagnetic radiation to obtain information, and to attempt to prevent hostile forces from doing the same. This leads to a succession of measures, countermeasures, and counter-countermeasures, all of which rely on complex electronic instrumentation and tactics for its use. EW permeates all aspects of modern warfare regardless of nationality, service affiliation, or location. It is no exaggeration to say that the successful conclusion of modern warfare depends heavily on EW.

Modern ships have Electronic Support Measures (ESM) equipment to detect other emitters and Electronic Countermeasures (ECM) equipment to deny the enemy the use of the electronic spectrum. The decision not to use electronic warfare or the inability to do so effectively, for whatever reason, can lead to disastrous results. The sinking of the British destroyer HMS Sheffield during the Faulklands Island dispute is an excellent example. The Sheffield was a sophisticated electronic picket-ship designed to protect the fleet. It was hit by a single radar-guided missile. The loss of the HMS Sheffield highlights the risks if electronic warfare principles are not effectively utilized in modern conflicts.

The same is true for air warfare. Without ECM, modern air defense could inflict unacceptable losses on an attacking force. This was demonstrated during the Vietnam conflict when the U.S. Air Force lost its first aircraft to hostile surface-to-air missiles. Increasing losses prompted a major countermeasures effort by the Department of Defense, the Joint Chiefs of Staff, the USAF and USN. ECM jamming pods and radar warning receivers were installed on tactical aircraft, and ECM support jamming aircraft were introduced. Aircraft carrying anti-radiation missiles were developed. As a result of these efforts, losses were greatly reduced. These are but two examples of many that illustrate the importance of Electronic Warfare.

There are three primary divisions of electronic warfare:

1. Electronic Warfare Support Measures (ESM);
2. Electronic Countermeasures (ECM);
3. Electronic Counter-Countermeasures (ECCM).

ESM can be defined as that division of electronic warfare involving actions taken to search for, intercept, locate and identify radiated electromagnetic energy. The purpose is immediate threat recognition for the use of ECM, ECCM, and tactical employment of forces.

ECCM involves actions taken to ensure friendly use of the electromagnetic spectrum despite the use of ECM by hostile forces.

ECM is the division of electronic warfare that prevents or reduces an enemy's effective use of the electromagnetic

spectrum. Electronic jamming is considered active ECM since the devices actively radiate energy. This is in contrast to passive ECM devices which do not actively radiate. Chaff, first used in World War II, is considered a passive ECM device. When ECM jammers are to be used to degrade the operation of hostile radars, there are many questions that confront the ECM planner: What type of jamming to use? At what altitude will the aircraft with self-protection jamming best penetrate the air defense? Where should a standoff jammer be positioned for maximum effectiveness? Etc.

Noise and deception jammers, which belong to the active electronic countermeasures category, radiate electromagnetic energy to degrade the operation of radars. Noise jammers were developed in World War II while deception jammers were developed later when wideband microwave amplifiers and oscillators became available.

Noise jammers increase the noise in the radar's bandpass to mask the reflected energy from the target. A noise-like signal is transmitted which has the same characteristic as the radar receiver's own internally generated noise. If sufficient noise is introduced, the target echo will not be distinguished by the radar operator.

Deception jammers confuse the radar operator by providing false range information, incorrect target-bearing information or many false targets. The deception jammer receives the radar signal and reradiates the signal after applying suitable

ECM modulation of amplitude, phase, frequency or time. The power output requirement of a deception jammer is less than a noise jammer. It is also possible to degrade the operation of the radar without betraying the fact that countermeasures are being employed.

Deception jammers use more sophisticated circuitry and techniques, and may be expected to be effective against only a specific class of radars. The noise jammer, on the other hand, provides some degradation to all types of radars. When the enemy realizes that noise jamming is present, electronic counter-countermeasures (ECCM) can be employed to obtain the information desired. Deception jammers are more difficult to counter.

This thesis discusses the correct positioning of an active ECM aircraft, using standoff or self-protection noise jammers. Antenna patterns of the threat radar and the jammer, and environmental conditions are considered. It is demonstrated that, with minor modifications, the Integrated Refractive Effects Prediction System (IREPS) has the capability to make the needed calculations for correct positioning.

Most tactical planning only takes the radar antenna pattern in the horizontal plane into account. This, in effect, leads to only considering a portion of the problem. Failure to consider the environment, and how it affects vertical positioning, can lead to substantially reduced jamming effectiveness and greater risks to the attacking force.

II. ANTENNA FACTORS IN POSITIONING JAMMING AIRCRAFT

A. RADAR SYSTEM

This section discusses the factors of a radar system that relate to the positioning of a jammer. The purpose of a radar system is the detection and location of targets. The radar emits electromagnetic energy and displays the target's range, altitude, azimuth, and velocity, or a combination of these, using the received reflected energy. The discussion here will be limited to pulsed radar systems, which use the same antenna for transmitted and received signals. Other systems are important, continuous wave radars for example, but they employ specialized processing techniques which are beyond the scope of this thesis.

A radar consists of three basic parts:

1. Transmitter
2. Receiver
3. Antenna

The transmitter sends out electromagnetic energy. The receiver intercepts, processes, and displays the energy reflected from the target. The antenna acts as the link between the radar system and the atmosphere. While the transmitter and receiver characteristics affect the range aspect of the positioning problem, the primary factor in determining the proper altitude and azimuth of the jammer is the radar antenna. Thus, the following discussion of radar systems will concentrate on the antenna.

The antenna has two basic functions: (1) to efficiently couple the transmitter or receiver to the atmosphere, or space, and (2) to focus the energy into an appropriately shaped beam. The radiation or antenna pattern is a plot of the relative intensity of the radiated energy as a function of the angle about the antenna. A spherical coordinate system is used to describe the antenna pattern (Figure 1). The horizontal-plane or azimuth pattern is determined by plotting

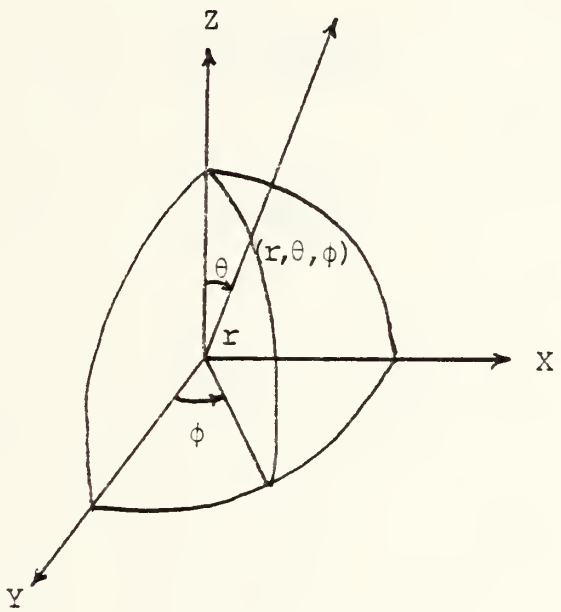

Figure 1. Spherical Coordinate System

relative energy as a function of ϕ in the X,Y plane. Similarly, the vertical-plane pattern is determined by holding ϕ constant and plotting relative energy as a function of θ. The term azimuth pattern and vertical or interference pattern

will be used to denote the horizontal-plane and vertical-plane patterns respectively.

In the past, the major consideration in the planning of standoff jamming has been the horizontal or azimuth positioning of the standoff jammer in relation to the attack aircraft. Figure 2 is a depiction of the azimuth positioning problem for an attack axis at zero degrees. The azimuth or horizontal-plane pattern (XY plane) is shown with the first sidelobe

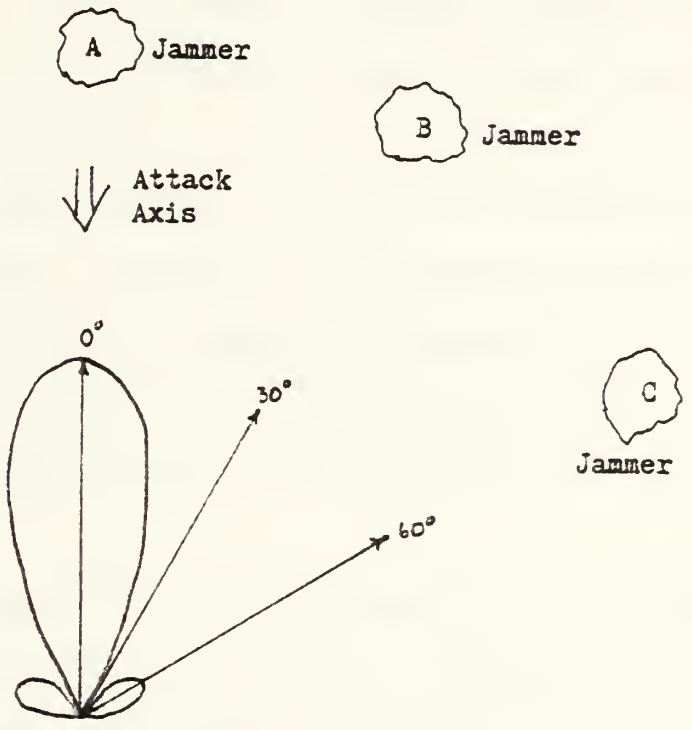

Figure 2. Aximuthal Positioning of a Standoff Jammer

(at 60 degrees) reduced about 8 db. Azimuth patterns depend on the shape of the antenna and are different for different

radars. Radars that perform different functions, such as search and tracking, will have greatly differing patterns. The proper positioning of the jammer depends upon the radar's antenna characteristics. To obtain the needed antenna information, the ECM planner would consult a warfare manual, which lists beam width, elevation angle, side-lobe location, and use that information to solve the azimuth positioning problem.

For example, if the standoff jammer is placed at point A in Figure 2, maximum jamming energy is introduced into the radar's receiver. At points B and C, assuming constant range the jamming energy at the radar's receiver is significantly reduced because the sensitivity of the radar antenna is reduced. At point B, theoretically, there is no jamming while at point C, the jamming is reduced 8 db compared to point A. It is important to note that, because of reciprocity, the antenna pattern is the same for both transmission and reception (if the same antenna is used to transmit and receive the radar signal).

The interference pattern (vertical pattern) of the radar is as important to the ECM planner as the azimuth pattern. An interference pattern, determined by holding ϕ constant and plotting relative energy as a function of θ (Figure 1) results when the energy from an antenna arrives at a point in space by two different paths. Figure 3 shows the multipath condition for a signal arriving at point E from direct and reflected paths over a reflecting flat surface.

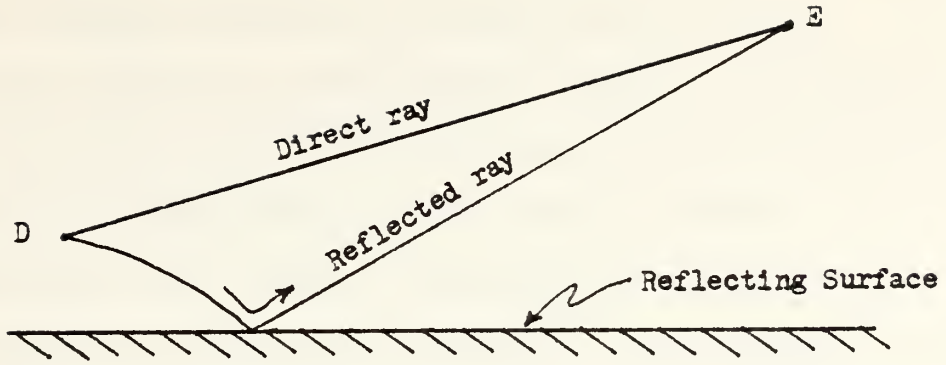

Figure 3. Direct and Reflected Paths over a Reflecting Surface

The interference calculation uses a reflecting spherical surface to account for the curvature of the earth, and a complex reflection coefficient to account for the fraction of incident energy reflected and the phase.

The signal strength at point E depends upon the amplitudes and phases of the direct and reflected waves. If the direct and reflected waves are in phase, a maximum occurs at point E, while if they are 180° out of phase a minimum occurs. Thus, for perfect reflection, the field strength at point E can vary from zero to twice the value that would exist if the reflecting surface were not present. The shape of the antenna which focuses the energy is a major factor in determining the interference pattern since it determines the angular dependence of the radiated energy.

Since different types of radars have different antenna shapes, some radars will have strong interference patterns while others may not. A search radar, whose purpose is to

keep a large vertical area under surveillance, has a broad vertical energy pattern and fixed elevation angle. If the reflecting surface is sufficiently smooth, the calculation of the interference pattern of the search radar is the microwave equivalent of the optical Lloyd's mirror effect.

Antennas with a fixed, high-elevation angle and low energy toward the reflecting surface (low sidelobes) would have negligible interference pattern. There would be no areas of reduced energy other than that produced by the antenna pattern. If the elevation angle of such a radar antenna is not fixed, the interference pattern will be dependent on the angle, which introduces additional complications.

For tracking radars, whose primary function is to supply position data for weapons control, the antenna will always be centered on the target (once acquired). Therefore, since the elevation angle varies with the target's location, the interference pattern would depend on the target location. Figure 4 shows a typical radiation pattern for a paraboloid reflector antenna used for tracking radars [Ref. 1]. A nearly symmetrical pencil-beam antenna pattern is generated by the paraboloid. If the antenna used to produce the pattern in Figure 4 were tracking a target at 10° elevation, little interference pattern would exist because there would be very little reflected energy due to the low sidelobes (-20 db at 10°) and high elevation angle. However, if the same paraboloid dish were tracking a target on the horizon, the interference

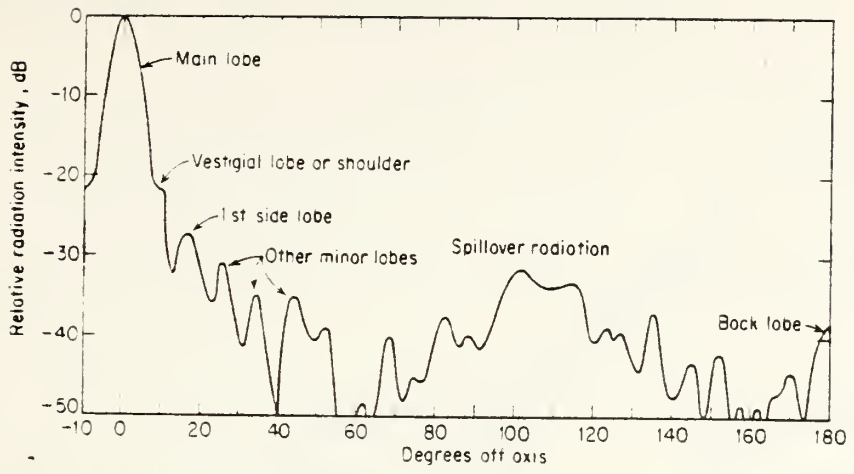

Figure 4. Typical Radiation Pattern of a Paraboloid Reflector Antenna

pattern could be significant. Strong interference maxima and nulls are factors the ECM planner should consider in the positioning problem.

The pattern-propagation factor, F, is used to account for both the antenna dependent interference pattern and the propagation effects that exist between antenna and target. Several non-free-space propagation factors can be included in F but abnormal refraction effects are the main considerations, and those we consider in this thesis.

F is the ratio of the field strength E, at a point in space, to that which would have been present, E_o, if free-space propagation had occurred and the point were in the antenna-pattern maximum [Ref. 2]. A pattern-propagation factor for each propagation path is used. F_t is defined as the pattern-propagation factor for the transmitting-antenna-to-target

path while F_r is defined as the factor for the target-to-receiving-antenna path (Figure 5).

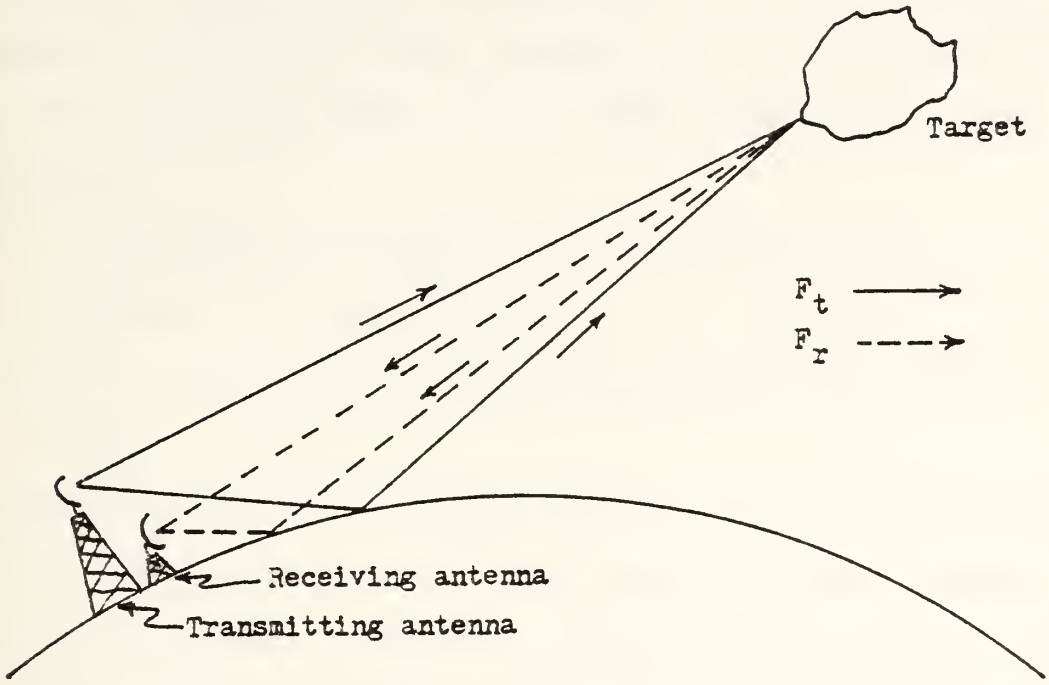

Figure 5. Pattern-Propagation Factors, F_t and F_r, for Transmitting and Receiving Paths

If the radar uses the same antenna for receiving and transmitting, F_t is equal to F_r. They are equal because of reciprocity and because the irregular surface of the target is assumed to radiate the reflected energy equally in all directions, that is, the target is treated as an omnidirectional antenna. The target is simply characterized by a radar cross section, σ, which is that flat area which would produce the same received signal as is actually observed from the aircraft.

B. JAMMING SYSTEM

The electromagnetic energy developed in the jamming transmitters, noise or deception, is directed to the radar through the ECM antenna. Regardless of which type of jamming is selected, noise, deception, or a combination of the two, the ECM antenna of the jammer system has these functions:

(1) to efficiently couple the transmitter to the atmosphere or space, and

(2) to focus the energy into an appropriately shaped beam.

The ECM antenna has an antenna pattern and the pattern depends on the type of the antenna, the same for a radar antenna discussed earlier. All of the considerations already discussed for a radar antenna apply to the jammer. The combined antenna pattern and propagation effects are described by the pattern-propagation factor F_j. If the jammer antenna is omnidirectional, $F_j = F_r$, since the target was assumed to radiate omnidirectionally. If a directional jammer is used, F_j must be calculated for the specific case of interest. This is not a simple matter since F_j will obviously depend on the aircraft altitude.

III. ENVIRONMENTAL FACTORS IN POSITIONING JAMMING AIRCRAFT

The environment is the total medium through which the radar and jamming signals propagate. It consists of the terrain and the atmosphere between the two systems. Environmental effects can substantially modify the propagation factors and can therefore be critical. It is necessary to divide the environment into two regions: the optical or interference, which is within the line of sight of the radar, and the diffraction region which lies beyond the horizon. Figure 6 is a curved earth depiction showing the two regions.

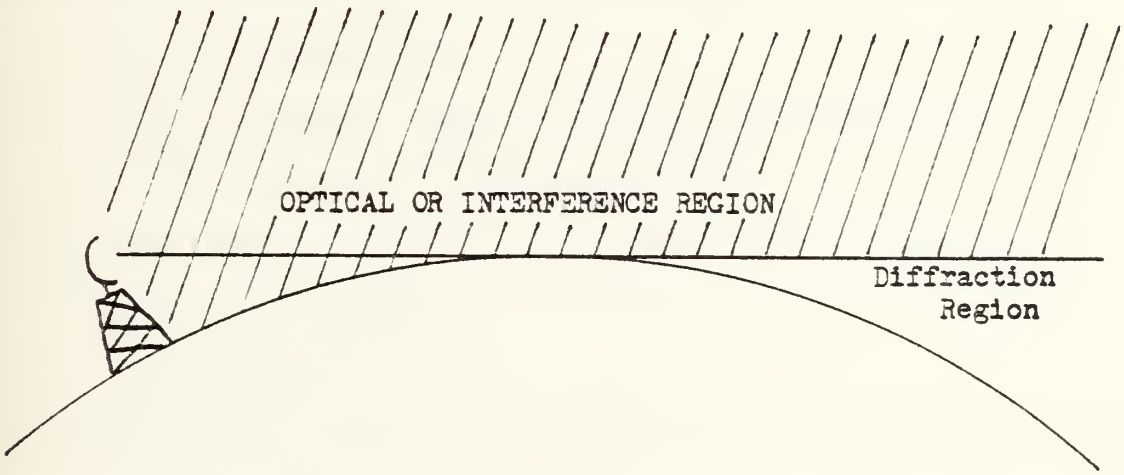

Figure 6. Curved-Earth Depiction of the Optical and Diffraction Regions

In the optical region, the important consideration is the interference pattern, while in the diffraction region the dominant effect is ducting. If ducting is not a factor, negligible energy enters the diffraction region.

A. OPTICAL REGION

To solve the interference problem, the reflection coefficient of the reflecting surface must be known. For a perfectly reflecting surface, the nulls in the lobe structure are at zero field strength since the direct and reflected signals are of equal amplitude. If the surface is rough, the nulls are "filled in" and the field strengths at the maxima are reduced. The determination of the specular reflection coefficient of a rough surface has not been fully solved [Ref. 3]. Significant work has been devoted to the solution of the problem and fair agreement has been achieved with rough-sea reflection experiments. The surface reflection coefficient depends on the following factors [Ref. 4]:

(1) surface roughness,

(2) grazing angle (angle between the ray and the surface at the reflection point),

(3) the complex dielectric constant of the material below the surface,

(4) polarization.

For military applications, the environment includes all types of overland terrain and all sea conditions. IREPS uses a modification of a formula given by Ament to predict the reflection coefficient of the ocean [Ref. 5]. The prediction of the reflection coefficient overland might be possible for certain geographical areas. If enough data were available to model a geographical area, say a flat desert region, then

the reflection coefficient could be used in an IREPS type model to predict the vertical energy pattern. For more complex terrain the problem is far from solved.

B. DIFFRACTION REGION

Energy enters the area beyond the horizon by diffraction and also by "anomalous" refraction. Radar waves can be diffracted in the same manner that light is diffracted by a straight edge. The amount of diffraction depends upon the size of the object compared to the wavelength of the wave. Diffraction is very important in very low frequency communication. However, at most radar frequencies, the wavelength is so small compared to the earth's dimension that diffraction is not a factor in extending the line of sight.

Refraction does have a significant effect on the propagation of radar beyond the horizon. Due to the vertical inhomogeneity of the atmosphere, radar waves are generally bent by refraction, which extends the distance of the horizon compared to the straight line or optical horizon (Figure 7). This

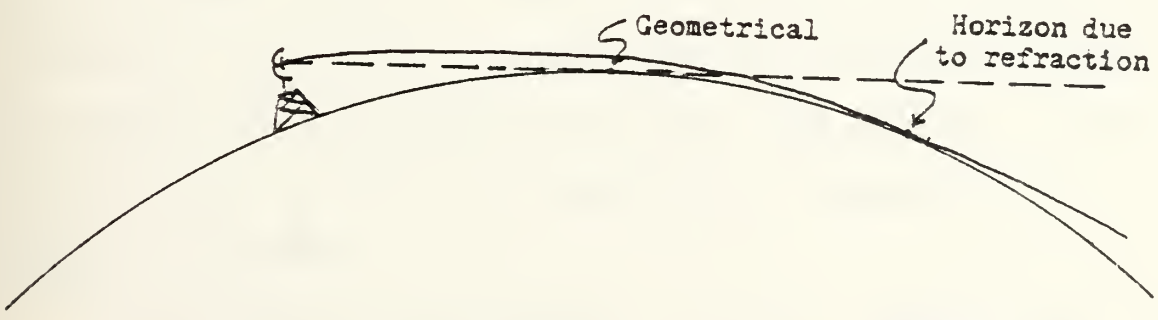

Figure 7. Horizon Extension Due to Refraction

bending is caused by variation of the velocity of propagation with altitude. The classical method of accounting for atmospheric refraction is to replace the actual earth of radius r with an equivalent earth of radius kr where k depends on conditions [Ref. 6]. In this coordinate system, the inhomogeneous atmosphere is replaced by a homogeneous atmosphere in which the radar waves propagate in straight lines rather than curved lines. The value of k used for a "standard atmosphere" is 4/3.

Refraction can cause an apparent elevation angle error in height-finder radars, but the most dramatic effects are caused by abnormal propagation or "ducting". A discussion of the mechanism of ducting is contained in Appendix A. The major effect of ducting on radars is to significantly increase radar range, extending the radar coverage beyond the horizon. Obviously, this is very important to the ECM planner. The IREPS User's Manual (see Appendix A) defines ducting as "the concentration of radio (or radar) waves in the lowest part of the troposphere in regions characterized by rapid vertical change in air temperature and/or humidity." This over-the-horizon radar coverage, caused by bending which exceeds the curvature of the earth, results when the atmospheric index of refraction, n, changes with height very rapidly. dn/dh is related to the vertical gradients of temperature and relative humidity.

By measuring the atmosphere's pressure, temperature, and water vapor pressure as a function of altitude, the amount

of bending can be calculated [Ref. 7]. The important consideration here is the gradient or rate of change of n with respect to altitude. If dn/dh is great enough, the radar rays follow the curvature of the earth. If the curvature of the earth is exceeded, the energy refracts down and then "bounces" upward from the reflecting surface many times (Figure 8).

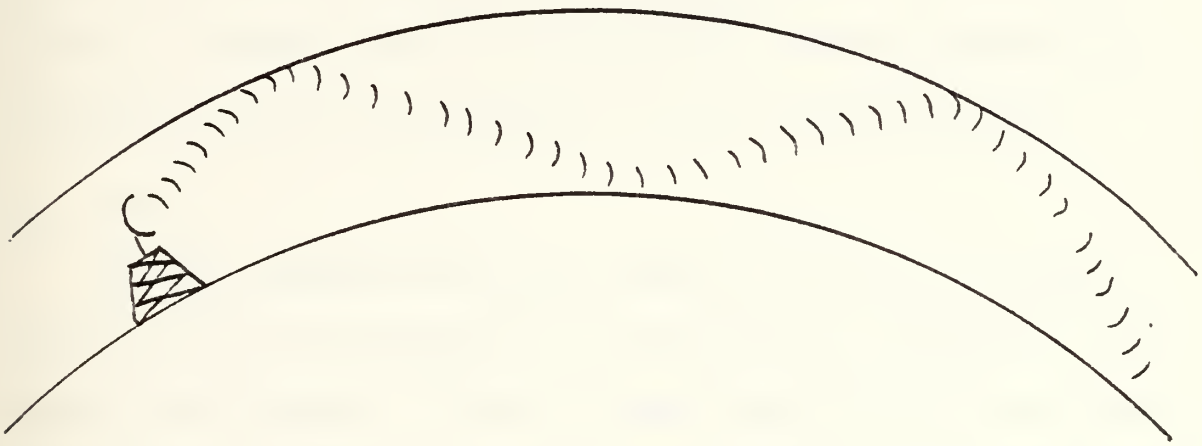

Figure 8. Ducting of Radar Waves and Over-the-Horizon Coverage

When ducting conditions are present, the location of the radar and ECM antennas with respect to the duct becomes an important consideration. Ducts can be used essentially as an extension of the antenna, carrying energy over long distances. Because of the shallow angle that is required to couple energy into the duct, the antenna must be close to or within the duct to use the duct effectively. The angle between the radar beam and the duct cannot normally be greater

than 1° or the energy passes through the duct and is not trapped [Ref. 8]. If the duct extends to the surface, surface or sea-based radars are strongly affected by its presence. Both the radar's and jammer's effective ranges can be extended by the duct. The jamming aircraft can only make use of this capability if it flies at an altitude that places it within the duct. If the ECM planner wishes to take advantage of ducting conditions, the location of the duct and the characteristics of the ECM antenna must be known. He then must be able to evaluate the over-the-horizon pattern-propagation factors in order to formulate the most effective plan.

C. IREPS

The Integrated Refractive Effects System can provide near real-time assessments of environmental conditions and system performance. IREPS has been specifically developed for the marine environment and the radar systems that operate in the environment. Path loss versus range plots and coverage diagrams are the two IREPS products of interest here. Coverage diagrams are vertical plane contours of constant received power plotted on a curved-earth presentation. The contour boundaries indicate received signal equal to minimum detection threshold. This minimum value is determined by a calculation based on the radars specified free-space range. The signal strength calculations include antenna pattern factors, reflection, and interference and refraction effects.

Coverage diagrams are provided for both long-range air-search radars employed against low-flying air targets [Ref. 9]. The path loss versus range diagrams indicate the loss, in db, as a function of range for a certain altitude target. For more details, see Appendix A.

IV. RADAR RANGE AND JAMMING EQUATIONS

A radar is designed to detect and locate targets and the jammer is designed to reduce the radar's ability to perform that task. Through the years, extensive efforts have resulted in the development of radar range and jamming equations that attempt to predict the performance of both systems. These predictions are not exact, however, they are very useful, and permit meaningful comparisons to be made of the relative performance of competing systems. Also, they are invaluable to the ECM planner in the development of tactics.

In analyzing radar and jammer performance, general practice in the past was to assume that the radar and target were both located in free space since non-free-space propagation effects are not easy to calculate. Graphs and monographs which simplify the calculations exist in the literature but such methods are not practical for tactical applications. The use of computers to perform the calculations has made it possible to easily and quickly evaluate non-free-space propagation factors.

In what follows, the radar range and jamming equations are developed and are written in simplified forms. The simplified forms allow one to easily identify the quantities that must be evaluated to take the environment into account. The developments of the radar range and self-protection jamming

equations follow from A Guide to Basic Pulse-Radar Maximum-Range Calculation, Part I--Equations, Definitions, and Aids to Calculations by Blake [Ref. 10].

A. RADAR RANGE EQUATION

The radar range equation predicts the maximum range at which a radar can detect a target. An understanding of the radar range equation is necessary since it is the basis for the jamming equations. By tracing the path of the energy from the radar transmitter, the development of the free-space radar range equation is straightforward.

The power, P_t (watts), generated by the transmitter is directed to the antenna through a transmission line. Transmission line losses reduce the power output to the antenna terminals to P_t/L_t where L_t is a loss factor defined as the ratio of the transmitter power output to that actually delivered to the antenna. For an isotropic antenna (radiates uniformly in all directions), the power density (watts per unit area) at a target located distance R from the antenna is:

$$\text{Power density at distance R (isotropic)} = \frac{P_t}{L_t 4\pi R^2} \quad (1)$$

However, radars use directional antennas and the power density at the target (directional antenna) is:

$$\text{Power density at distance R (directional)} = \frac{P_t G_t}{L_t 4\pi R^2} \quad (2)$$

where G_t is the on-axis transmitting antenna gain. The radiated energy strikes the target and the energy reradiated is the incident power density times the target "radar cross section", σ. The power density at the receiving antenna is:

$$\text{Power density at receiving antenna} = \frac{P_t G_t}{L_t 4\pi R^2} \sigma \frac{1}{4\pi R^2}. \quad (3)$$

The receiving antenna collects that portion of the energy that falls on its effective area, A_e. Thus, the received power, P_r, is:

$$P_r = \frac{P_t G_t}{L_t 4\pi R^2} \sigma \frac{A_e}{4\pi R^2}. \quad (4)$$

The relationship between the receiving antenna gain G_r and the antenna's effective area, A_e, of a lossless antenna is [Ref. 11]:

$$G_r = \frac{4\pi A_e}{\lambda^2}. \quad (5)$$

Equation 5 can be substituted into Equation 4 to give:

$$P_r = \frac{P_t G_t}{L_t 4\pi R^2} \sigma \frac{1}{4\pi R^2} \frac{G_r \lambda^2}{4\pi}. \quad (6)$$

If the same antenna is used for transmission and reception, $G_r = G_t$.

By solving for R, Equation 6 becomes a range equation:

$$R^4 = \frac{P_t}{P_r} \frac{G_t G_r \sigma \lambda^2}{(4\pi)^3 L_t} \tag{7}$$

Note that the target range can be determined if P_t/P_r is known since all other factors are constant. (The value of the cross section, σ, for the target of interest must be available.) If P_r is replaced by $P_{r(min)}$, the minimum detectable value, the equation gives the maximum range for detection:

$$R_{fs}^4 = \frac{P_t G_t G_r \sigma \lambda^2}{P_{r(min)} (4\pi)^3 L_t}. \tag{8}$$

R_{fs} is the free-space radar range since no environmental factors are included in Equation 8.

$P_{r(min)}$ can be shown to be:

$$P_{r(min)} = (S/N)_{min} \, k \, T_s \, B_n, \tag{9}$$

where:

$(S/N)_{min}$ is the minimum signal-to-noise ratio for detection,

k is Boltmann's constant,

T_s is the receiving system noise temperature,

B_n is the noise bandwidth of the receiver.

Therefore, the free-space range is:

$$R_{fs}^4 = \frac{P_t G_t G_r \sigma \lambda^2}{(S/N)\, k\, T_s\, B_n\, (4\pi)^3\, L_t}, \qquad (10)$$

where we drop the subscript on (S/N) for convenience. There are many losses which have not been considered in this development. A convenient approach is to use a generalized loss factor, $L = L_t L_1 L_2 \cdots$, in the denominator of Equation 10. $L_1, L_2, \ldots$ are additional loss factors (besides L_t) that are determined to be significant in reducing radar energy. Discussions on loss factors can be found in [Ref. 12] and [Ref. 13]. We will substitute L for L_t in what follows.

Equation 10 is valid for a consistent system of units, but the use of "mixed" units, such as nautical miles for range, square meters for target cross section, kilowatts for transmitter power, etc., is more convenient. It is also more convenient to express the wavelength λ in terms of equivalent frequency in megahertz, the noise temperature in terms of the noise figure, and the receiving bandwidth as a function of pulse length. These substitutions are:

$$T_s = 290\, N_f, \qquad (11)$$

$$B_{KHz} = 1000/\tau, \qquad (12)$$

$$\lambda = c/f, \qquad (13)$$

where:

N_f is the noise figure (unitless),

τ is the pulse length in microseconds,

f is the frequency in megahertz,

c is the speed of light (m/sec).

Combining all constants and unit conversions into a single constant gives:

$$R_{fs} = 31.32 \left[\frac{P_{t(kw)} G_t G_r \sigma_{(sq\ m)} \tau_{(microseconds)}}{f^2_{(MHz)} N_f (S/N) L}\right]^{1/4}. \quad (14)$$

The pattern-propagation factors, accounting for non-free-space propagation, interference, and the fact the target may not be in the antenna-pattern maximum, reduces or enhances the transmitted or reflected power. Including the pattern-propagation factors, F_t and F_r, in Equation 14 gives:

$$R_{max} = 31.32\ F_t^{1/2}\ F_r^{1/2} \left[\frac{P_t G_t G_r \sigma \tau}{f^2 N_f (S/N) L}\right]^{1/4}, \quad (15)$$

where:

R_{max} is the maximum radar detection range in nautical miles,

F_r is the pattern-propagation factor for the target-to-receiving-antenna path,

F_t is the pattern-propagation factor for the transmitting-antenna-to-target path.

Two conditions have to be satisfied if $F_t = F_r$. The same antenna has to be used for the transmitted and received signal and the target has to reflect the transmitted energy omnidirectionally. For the radars considered in this thesis, the same antenna is used to transmit and receive the energy. The subscript "max" denotes that non-free-space as well as free-space factors are considered in the equation. If only free-space factors are considered, the subscript "fs" will be used.

It is illustrative to rewrite Equation 15 as:

$$R_{max} = F_t^{1/2} F_r^{1/2} R_{fs} . \qquad (16)$$

This equation shows that the free-space behavior and propagation factors can be calculated separately. For a particular radar and target, R_{fs} is a constant that can be precalculated. Note that R_{fs} assumes that the target is "on-axis" for the transmission and receiver antenna patterns.

B. JAMMING EQUATIONS

Tactical employment of jammers can be divided into three scenarios:

(1) Self-protection jamming

(2) Standoff jamming

(3) Escort jamming

Standoff and escort jamming are support ECM tactics; their effectiveness depends on the location of the jamming platform

with respect to both other friendly vehicles and the enemy radar system.

Self-protection or self-screening jamming is where the platform carries a jammer to protect itself from threatening enemy electronic systems. Self-protection jamming is generally associated with fighter-type aircraft using noise or deception jamming against threat radars. Since the jammer is located on the target platform, only target and radar locations need be considered.

Standoff jamming is a support jamming technique where the jamming platform remains close to, but outside of, the lethal range of the enemy defense system. It is generally employed against search and acquisition radars. The large radar-to-jammer range and alignment problem reduces the effectiveness of a standoff jammer against tracking radars.

For escort jamming, the jamming platform accompanies the strike aircraft and is within lethal range. If the escort platform flies in cell with the strike aircraft, so that both are located in the main beam of the radar at the same time, the self-protection jamming equation is applicable. If the escort jamming platform does not fly in cell with the strike aircraft, the problem is essentially the same as for standoff jamming. Thus, there are no equations especially derived for escort jamming. Modifications of the self-protection or standoff jamming equations can be made when employing escort jamming.

1. Self-Protection Noise-Jamming Equations

The noise jammer produces a signal that adds to the already present thermal noise in the radar receiver. The received jamming signal power spectral density, P_{rj}, watts per hertz, is given by:

$$P_{rj} = \frac{P_j G_j G_r \lambda^2 F_j^2}{(4\pi R_j)^2 L_j}, \qquad (17)$$

where:

P_j is the jammer power spectral density in watts per hertz,

G_j is the jammer antenna power gain,

F_j is the pattern-propagation-factor for the jammer-to-radar path,

R_j is the jammer-to-radar range,

L_j is assumed system losses (unitless).

By substitution of P_{rj} for kT_s in the maximum range equation (Equation 18), the self-protection noise-jamming equation is derived. The correct substitution is $(P_{rj} + kT_s)$ for kT_s but, the received-jamming signal is assumed much larger than receiver noise so kT_s is dropped. Thus

$$R_{max}^4 = \frac{P_t G_t G_r \sigma \lambda^2 F_t^2 F_r^2}{(S/N)\ kT_s\ B_n\ L_r\ (4\pi)^3} \qquad (18)$$

becomes

$$R_{max}^4 = \frac{P_t G_t G_r \sigma \lambda^2 F_t^2 F_r^2}{(S/N) B_n L_r (4\pi)^3} \left[\frac{P_j G_j G_r \lambda^2 F_j^2}{(4\pi R_j)^2 L_j} \right]^{-1} . \qquad (19)$$

In Equations 18 and 19, respectively, L_r replaces L for the radar signal losses and L_j replaces L for the jammer signal losses. (If F_j^2 is small, then P_{rj} is approximately equal to kT_s and substitution of $(P_{rj} + kT_s)$ for kT_s would be required.) The resulting equation for the self-protection case is:

$$\frac{R_{max}^4}{R_{max}^2} = \frac{P_t G_t \sigma F_t^2 L_j F_r^2}{(S/N) B_n P_t G_j 4\pi L_r F_j^2} , \qquad (20)$$

where R_{max} is the maximum distance the target can be detected in the presence of jamming noise.

One additional term in Equation 20 is required when the polarization of the jamming system does not match that of the radar system: L_p, the polarization loss factor. It was not needed in the radar range equation because the polarization of the transmitting and receiving antennas are the same. If the jammer and the radar have the same polarization, L_p is equal to unity. For all other cases, the polarization loss factor is less than one. For a circular polarized jammer antenna and a linear polarized radar antenna, L_p is 1/2. Theoretically, the loss is infinite for the case where the jamming antenna and the radar antenna are perfectly crosspolarized.

With the inclusion of the polarization loss factor in the numerator and by expressing Equation 20 in convenient units, substitution of Equation 12 for B_n, and collecting all the constant terms, the self-protection noise-jamming equation becomes:

$$SPJ_{max} = 4.187 \times 10^{-3} \frac{F_r F_t}{F_j} \times \left[\frac{P_{t(KW)} \tau_{(microseconds)} \sigma_{(sq.m.)} G_t L_p L_j}{P_t G_j (S/N) L_r} \right]^{1/2}, \quad (21)$$

where:

SPJ_{max} is the maximum burnthrough range, in nautical miles, when self-protection noise-jamming is present. As in the radar range equation, the subscript "max" denotes that non-free-space factors are considered.

The burnthrough range is the maximum radar-to-target slant range for which the radar receiver can detect the reflected energy of the incoming target in the presence of the jammer noise. The term "burnthrough" is used because, as the target approaches the radar, the radar signal will burn through the jammer noise when the range SOJ_{max} is reached and target detection will result.

The burnthrough equation can be rewritten as:

$$SPJ_{max} = \frac{F_t F_r}{F_j} SPJ_{fs}, \quad (22)$$

where:

SPJ_{fs} is the free-space burnthrough range, in nautical miles, when self-protection noise-jamming is present and

$$SPJ_{fs} = 4.187 \times 10^{-3} \left[\frac{P_t \tau G_t \sigma L_p L_j}{P_t G_j (S/N) L_r} \right]^{1/2} . \qquad (23)$$

The constant free-space parameters can be pre-evaluated and the changing environmental conditions are contained in the pattern-propagation factors.

2. Standoff Noise-Jamming Equation

For the standoff jamming case, the geometry of the jamming and attack aircraft with respect to the radar is shown in Figure 2. The amount of reflected energy from the attack aircraft received by the receiver is given by Equation 6. With the inclusion of the loss and pattern-propagation factors, Equation 6 becomes:

$$S = \frac{P_t G_t G_r \sigma \lambda^2 F_t^2 F_r^2}{(4\pi)^3 R_t^4 L_r} , \qquad (24)$$

where:

S is the received radar energy from the target, and

R_t is the radar-to-target range.

All other terms are the same as those used in Equation 15. The noise from the standoff jammer is:

$$N = \frac{P_j B_n G_{jr} G_{rj} F_j^2 \lambda^2}{(4\pi)^2 R_j^2 L_p L_j} , \qquad (25)$$

where:

N is the noise injected into the radar receiver,

G_{jr} is the gain of the jammer antenna toward the radar,

G_{rj} is the gain of the radar antenna toward the jammer,

and the other terms are the same as defined in Equation 17. G_{jr} and G_{rj} contain azimuthal factors while the elevation considerations are contained in the pattern-propagation factors. The radar receiver signal-to-noise ratio is:

$$\frac{S}{N} = \frac{P_t G_t G_r \sigma F_t^2 F_r^2 R_j^2 L_p L_j}{4\pi R_t^4 P_j B_n G_{jr} G_{rj} F_j^2 L_r} . \qquad (26)$$

Solving for R_t

$$R_t^4 = \frac{P_t G_t G_r \sigma F_t^2 F_r^2 R_j^2 L_p L_j}{4\pi \left(\frac{S}{N}\right) P_j B_n G_{jr} G_{rj} F_j^2 L_r} \qquad (27)$$

and by replacing R_t with R_{max} and (S/N) with $(S/N)_{min}$, the maximum range equation with standoff jamming is:

$$SOJ_{max}^4 = \frac{P_t G_t G_r \sigma F_t^2 F_r^2 R_j^2 L_p L_j}{4\pi \left(\frac{S}{N}\right) P_j B_n G_{jr} G_{rj} F_j^2 L_r} , \qquad (28)$$

where SOJ_{max} is the maximum burnthrough range with standoff noise jamming present.

Separating Equation 27 into free-space and propagation factors:

$$SOJ_{max}^4 = \frac{F_t^2 F_r^2}{F_j^2} SOJ_{fs} , \qquad (28)$$

where SOJ_{fs}, the free-space burnthrough range when standoff noise jamming is present, is:

$$SOJ_{fs} = \frac{P_t G_t G_r \sigma R_j^2 L_p L_j}{4\pi \left(\frac{S}{N}\right) P_j B_n G_{jr} G_{rj} L_r} . \qquad (30)$$

All of the symbols used have been defined as they were introduced. However, since there are a large number, a complete list follows for the reader's convenience.

P_t - transmitter power,

L_t - ratio of the transmitter power output to that actually delivered to the antenna,

R - radar-to-target range,

G_t - transmitting antenna gain,

σ - radar cross section,

A_e - effective area of receiving antenna,

P_r - received power,

S/N - minimum signal-to-noise ratio for detection,

kT_s - Boltzmann's constant times the receiving noise temperature,

B_n - noise bandwidth of the receiver,

G_r - receiving antenna gain,

N_f - noise figure of the receiver,

τ - pulse length,

f - frequency,

c - speed of light,

F_t - pattern-propagation factor for the transmitting-antenna-to-target path,

F_r - pattern-propagation factor for the target-to-receiving-antenna path,

R_{max} - maximum radar detection range (including non-free-space factors),

R_{fs} - free-space radar detection range,

P_{rj} - received jamming signal power spectral density,

P_j - jammer power spectral density,

G_j - jammer antenna gain,

F_j - pattern-propagation-factor for the jammer-to-radar path,

R_j - jammer-to-radar-range,

L_p - polarization loss factor,

L_j - jammer system losses,

L_r - radar system losses,

SPJ_{max} - maximum self-protection burnthrough range (includes non-free-space factors),

SPJ_{fs} - free-space self-protection burnthrough range,

S - received radar energy,

R_t - radar-to-target range,

N - noise injected into the radar receiver,

G_{jr} - gain of the jammer antenna toward the radar (azimuthal),

G_{rj} - gain of the radar antenna toward the jammer (azimuthal),

SOJ_{max} - maximum standoff burnthrough range (includes non-free-space factors),

SOJ_{fs} - free-space standoff burnthrough range.

V. ECM TACTICS PLANNING

The ECM planner, desiring to optimize the location of available jamming assets, has few aids to assist him. The available jamming equations, while accounting for azimuth positioning, generally do not consider vertical positioning. This section outlines a step-by-step approach for using IREPS and the jamming equations to assist the ECM planner in this task.

After inputting environmental and radar information into IREPS, the planner can obtain coverage diagrams which provide him with the radar's areas of detection without jamming present. This graphical presentation provides initial detection information and jamming initiation estimates. Modified coverage diagrams, which use values derived from the self-protection and standoff jamming equations, can provide graphical presentation of the jammer effects on the radar. Modified loss displays could provide the pattern-propagation factors needed to solve the jamming equations.

The pattern-propagation factors, critical to the vertical positioning problem, appear in the radar range and jamming equations in various forms. Table I lists these forms for the radar range, self-protection and standoff jammer cases.

A. ENVIRONMENTAL INFORMATION

Environmental effects include both the terrain and the atmosphere. In IREPS, the terrain used is the marine

TABLE I

Forms of the Pattern-Propagation Factors

(F) For Special Cases

GENERAL CASE

$X_{max} = (F)\ X_{fs}$

X_{max}	(F)	X_{fs}	Radar uses same antenna for transmitting and receiving Ⓐ		Radar uses different antenna for transmitting and receiving	
			Omnidirectional Jammer Antenna	Directional Jammer Antenna	Omnidirectional Jammer Antenna	Directional Jammer Antenna
SPJ_{max}	$\frac{F_t F_r}{F_j}$	SPJ_{fs}	F_t	$\frac{F_t^2}{F_j}$	F_t	$\frac{F_t F_r}{F_j}$
SOJ_{max}	$\frac{F_t^{\frac{1}{2}} F_r^{\frac{1}{2}}}{F_j^{1/2}}$ *	SOJ_{fs}	$\frac{F_t}{F_j^{1/2}}$	$\frac{F_t}{F_j^{1/2}}$	$\frac{F_t^{\frac{1}{2}} F_r^{\frac{1}{2}}}{F_j^{1/2}}$	$\frac{F_t^{\frac{1}{2}} F_r^{\frac{1}{2}}}{F_j^{1/2}}$
R_{max}	$F_t^{\frac{1}{2}} F_r^{\frac{1}{2}}$	R_{fs}	F_t		$F_t^{\frac{1}{2}} F_r^{\frac{1}{2}}$	

*Note: R_j is included in SOJ_{fs}

Ⓐ $F_t = F_r$

Radar uses same antenna for transmitting and receiving $\Longleftrightarrow$ $F_t = F_r$

Self-protection omnidirectional jamming antenna $\Longleftrightarrow$ $F_r = F_j$

environment with the conductivity and dielectric constant of sea water used for the surface. The reflection coefficient and surface roughness are developed for this case, and they vary with wave height, which is a function of wind speed [Ref. 14]. Therefore, IREPS, as presently configured, is limited to shipborne radars or land-based radars overlooking a marine environment.

The atmospheric effects are determined by microwave refractometer and/or radiosonde. The radiosonde directly measures temperature, humidity, and pressure which are used to calculate refractivity. The radiosonde is balloon-borne while the microwave refractometer can be installed on aircraft flying altitude profiles. Thus, both provide refractivity as a function of height and can be used as inputs for IREPS. The IREPS User's Manual, Appendix A, discusses the entering of environmental data.

After the environmental data is entered into IREPS, a propagation conditions summary and environmental data list are available as outputs. Figure 9 is a propagation condition summary for actual radiosonde data from the USS Nimitz for a weak surface-based duct. Figure 10 is the associated environmental data list used for checking numerical values of the data entries. The propagation conditions summary shows the presence and vertical extent of any ducts. The location, date/time, and a plain language narrative assessment of propagation effects are also provided.

IREPS REV 2.0

**** PROPAGATION CONDITIONS SUMMARY ****

LOCATION: NIMITZ
DATE/TIME: 2333Z 8 FEB 80 (N)

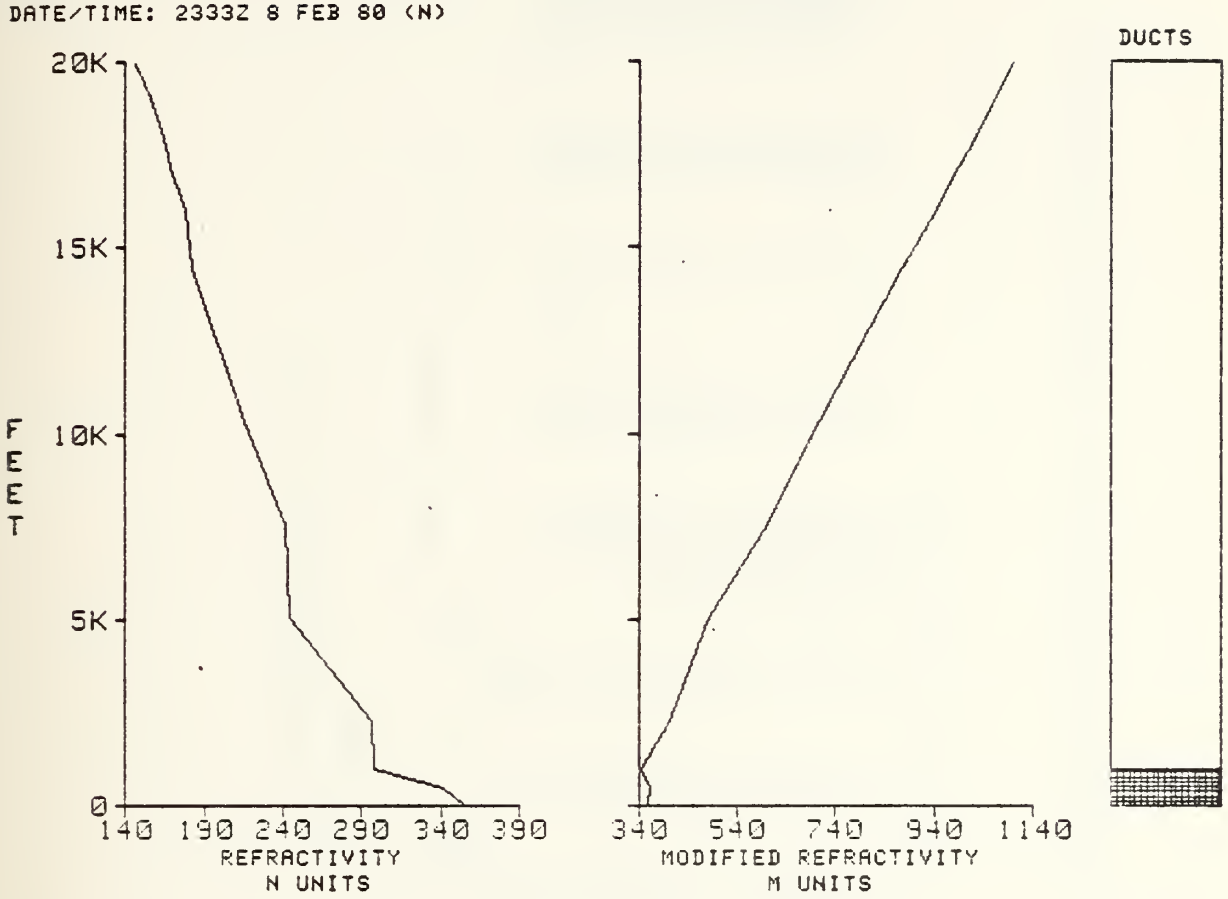

WIND SPEED= 5.0 KNOTS

SURFACE-TO-SURFACE
EXTENDED RANGES AT ALL FREQUENCIES

SURFACE-TO-AIR
EXTENDED RANGES FOR ALTITUDES UP TO 996 FEET
POSSIBLE HOLES FOR ALTITUDES ABOVE 996 FEET

AIR-TO-AIR
EXTENDED RANGES FOR ALTITUDES UP TO 996 FEET
POSSIBLE HOLES FOR ALTITUDES ABOVE 996 FEET

SURFACE REFRACTIVITY: 356 --SET SPS-48 TO 344

Figure 9. Propagation Condition Summary for a Weak Surface-Based Duct

IREPS REV 2.0

**** ENVIRONMENTAL DATA LIST ****

LOCATION: NIMITZ
DATE/TIME: 2333Z 8 FEB 80 (N)

WIND SPEED 5.0 KNOTS SURFACE PRESSURE = 1014.7 mB
RADIOSONDE LAUNCH HEIGHT = 32.8 FEET

LEVEL	PRESS (mB)	TEMP (C)	RH (%)	DEW PT DEP(C)	FEET	N UNITS	N/Kft	M UNITS	CONDITION
1	1,014.7	22.2	78.0	4.0	32.8	356.1	-35.8	357.6	SUPER
2	1,000.0	21.0	72.0	5.2	449.2	341.2	-79.9	362.7	TRAP
3	981.0	22.8	34.0	16.8	996.0	297.5	-.6	345.1	NORMAL
4	938.0	19.8	48.0	11.3	2,269.6	296.7	-19.3	405.3	NORMAL
5	850.0	15.6	19.0	30.0	5,031.4	243.5	-.9	484.2	NORMAL
6	775.0	9.1	52.0	9.3	7,571.5	241.2	-9.6	603.4	NORMAL
7	700.0	4.8	47.0	10.4	10,318.3	214.9	-8.1	708.6	NORMAL
8	598.0	-4.3	39.0	12.0	14,463.1	181.5	-2.6	873.4	NORMAL
9	563.0	-8.1	72.0	4.1	16,012.4	177.5	-8.1	943.5	NORMAL
10	538.0	-10.0	62.0	5.9	17,166.8	168.2	-4.8	989.4	NORMAL
11	521.0	-13.0	72.0	4.0	17,975.2	164.3	-8.2	1,024.3	NORMAL
12	500.0	-15.0	53.0	7.5	19,000.8	155.9	-10.2	1,065.0	NORMAL
13	481.0	-13.8	19.0	30.0	19,964.7	146.1	------	1,101.3	------

SURFACE REFRACTIVITY: 356 --SET SPS-48 TO 344

Figure 10. Environmental Data List for a Weak Surface-Based Duct

B. RADAR AND ECM INFORMATION

Detailed radar and jamming system parameters are required for inclusion in IREPS and solving the jamming equations. Just a few of the parameters required are: (1) transmitter and receiver characteristics of the radar, such as, power output, frequency, noise figure of the receiver, and associated transmitter and receiver losses, (2) antenna characteristics, such as, antenna height, antenna pattern, elevation angle, and vertical beamwidth, and (3) the target radar cross section. The jamming system parameters which would be needed are basically the same. A comprehensive listing of required parameters can be obtained from the jamming equations and IREPS input requirements.

Free-space radar range and jamming equations have been used for many years. Thus, the required radar and ECM information is readily available in classified technical and operating manuals for our systems and in classified intelligence documents for hostile systems. Therefore, the appropriate radar and jamming system parameters could be contained in IREPS files and the ECM planner could select the appropriate threat and the ECM system from a menu. IREPS currently does not contain any jamming system characteristics but does contain files where classified radar information can be stored (see Appendix A).

C. IREPS COVERAGE AND LOSS DISPLAYS

A coverage display is a curved-earth range-versus-height plot where the shaded area indicates the probable area of

detection. Figure 11 is a coverage display for a ficticious low-altitude acquisition-type radar (labled A) using the propagation conditions from the USS Nimitz (Figures 9 and 10). Table II lists the parameters for radar A. It is important to note that points all along the edge of the coverage diagram have the same field strength, while inside the shaded area, the field strength is greater but the exact value is not known. The boundary received signal strength is the minimum detectable value.

TABLE II

Radar A Parameters

```
LINE
  1  NAME OF COVERAGE DIAGRAM IS RADAR A EL 1
  2  TYPE OF DISPLAY IS USER REQUEST AT RUN TIME
  3  TYPE OF PLATFORM IS SURFACE
  4  ANTENNA HEIGHT =    25.0 FEET
  5  FREQUENCY =  1000 MHZ
  6  FREE SPACE RANGE =     80 NAUTICAL MILES
  7  ANTENNA TYPE IS SINX/X
  8  VERTICAL BEAM WIDTH = 4.0 DEGREES
  9  ANTENNA ELEVATION ANGLE =   1 DEGREES
 10  SECURITY CLASSIFICATION IS UNCLASSIFIED
 11  LABEL:
RADAR A
EL 1 BEAMWIDTH 4
```

Critical ECM planning information is available from the coverage diagrams. Figure 11 shows that detection of an aircraft flying at 10,000 feet would occur at 120 nautical

IREPS REV 2.0

**** COVERAGE DISPLAY ****

RADAR A EL 1

LOCATION: NIMITZ
DATE/TIME: 2333Z 8 FEB 80 (N)

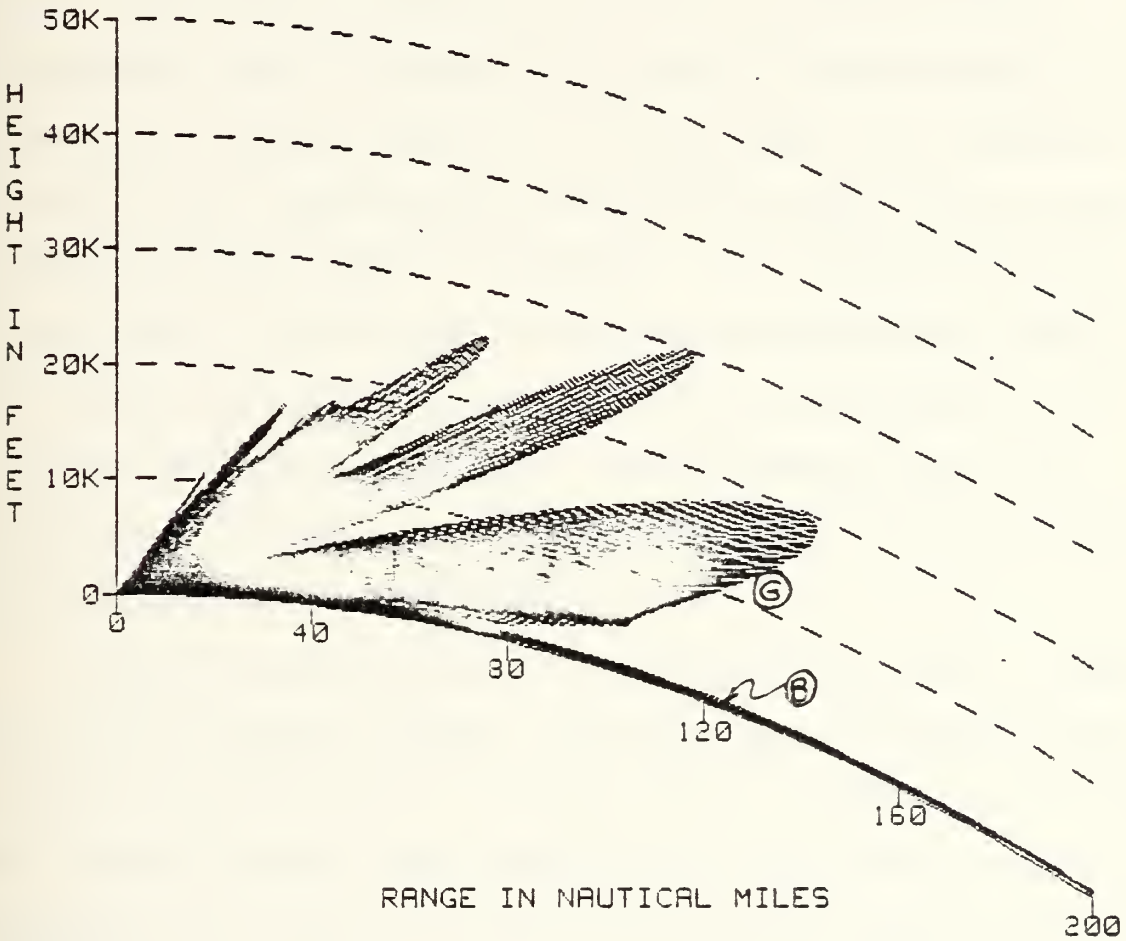

RADAR A
EL 1 BEAMWIDTH 4

SHADED AREA INDICATES AREA OF DETECTION OR COMMUNICATION

FREE SPACE RANGE: 80.0 NAUTICAL MILES
FREQUENCY: 1000 MHZ
TRANSMITTER OR RADAR ANTENNA HEIGHT: 25.0 FEET

Figure 11. 200 Nautical Mile Radar A Coverage Diagram for a Weak Surface-Based Duct

miles (Point G, Figure 11). This is also when initiation of active ECM should begin.

An understanding of the free-space range listed at the bottom of the coverage diagram is important. If the free-space range value is based on the free-space radar range equation, the coverage display is a radar coverage display which shows areas of detection with no jamming present. The free-space range could also be based on the free-space self-protection jamming equation. In that case, the coverage display shows the detection area of the radar for the given self-protection jamming conditions. The coverage display could then be called a self-protection burnthrough display. The same reasoning could be used for the development of a standoff burnthrough display. IREPS presently does not distinguish between the coverage displays but the distinction will be used in what follows.

The pattern-propagation factors are calculated in IREPS but are not normal outputs. The path-loss calculation was modified for this work to output pattern-propagation factors for various ranges. This modification was necessary to determine the value of F_j for the standoff jamming problem.

D. PLANNING THE MISSION

1. Self-Protection Noise-Jamming

The following is a step-by-step method for determining the optimum altitude for a self-protection noise-jammer:

1. Obtain needed environmental, radar and jammer information.
2. Select the coverage display option in IREPS to generate the radar coverage diagram. The radar coverage diagram is important to the ECM planner since it provides an indication of the best altitude to delay detection. The selection of the penetration altitude determines the range where probable detection occurs. Jamming should be initiated at the probable detection position.
3. Select the coverage display option in IREPS to generate the self-protection burnthrough coverage diagram. The value of Equation 23, SPJ_{fs}, is used as the free-space range. The ECM planner uses the self-protection burnthrough coverage diagram to determine the range where burnthrough occurs. A different altitude might be selected for this portion of the flight to reduce burnthrough range. Therefore, a preplanned mission might involve commencing jamming at one altitude and flying at a different altitude to delay burnthrough.
4. The preplanned flight path with penetration altitudes and jamming turn-on ranges are completed for a specific radar. The process can be repeated for another radar.

For target tracking radars at elevation angles greater than 3 to 5 degrees, the non-free-space effects can be neglected [Ref. 15]. Minimal multipath effects occur at those angles because the vertical sidelobes are significantly reduced. The pattern-propagation factors can be set to unity

and the equations solved without using IREPS. Below 3 to 5 degrees, IREPS should be used to determine if an optimum attack altitude can be found.

2. Standoff Noise-Jamming

The determination of the optimum location for the standoff jammer using IREPS is similar to the self-protection case. The standoff jamming equation has more factors and involves the determination of F_j, the pattern-propagation factor for the jammer-to-radar path. Equation 28 is used to determine the optimum altitude and range for the standoff jammer. For ease of calculation, Equation 28 is arranged similarly to the standoff jamming equation developed by Blake [Ref. 16]. The rearranged equation is

$$SOJ_{max(n.m.)} = F_t \left[6.94\times10^{-2} \left(\frac{P_{t(kw)} \tau_{(\mu s)} G_t G_r \sigma_{(sq.m)} L_p L_j}{P_{j(w/MHz)} G_{jr} G_{rj} \left(\frac{S}{N}\right) L_r} \frac{R^2_{j(n.m.)}}{F_j^2} \right)^{\frac{1}{4}} \right] . \quad (31)$$

F_t refers to the radar-to-target path and R_j^2/F_j^2 to the jammer-to-radar path.

To achieve maximum jamming (minimum value of SOJ_{max}) the optimum azimuthal and vertical positioning is required. For a fixed azimuth position (which fixes G_{rj}), F_j and R_j are the only jammer terms which vary with range and altitude. Therefore, if the ratio of R_j^2/F_j^2 is minimized, the minimum value of burnthrough, with respect to jammer location, is achieved. For a fixed standoff range, R_j, the largest value

of F_j would give the best results. If a plot of R_j^2/F_j^2 versus altitude for a given range were available, the altitude determination would be quite easy. The path-loss display was modified for this work to provide the pattern-propagation factor, F^2, versus range for a given altitude. This was useful in obtaining results in the next section; however, examination of Equation 31 shows the important relationship is R_j^2/F_j^2, which could be easily provided. Thus, for a pre-specified altitude, the F^2 factor is listed for many ranges. The determination of the F^2 factor at a certain range is straightforward, but the determination of the minimum value of R^2/F^2 is awkward. The altitude where F_j is largest is not readily apparent from the coverage diagram, but a general rule is that the largest value occurs along the main lobe of the interference pattern of the radar. Any surface-based duct should also be considered due to the trapped energy.

The method for determining the optimum location for the standoff noise-jammer starts with obtaining the needed information, as in the self-protection case. The following are the steps required:

1. Same as Step 1 in the self-protection case.
2. Generate radar coverage diagram to determine probable detection position for attacker and jamming initiation. This also gives the approximate altitude of the main lobe of the interference pattern for a first estimate of jammer altitude.

3. Use radar coverage diagram from Step 2 to select range(s) and altitude(s) to use in the path-loss displays.
4. Run path-loss displays to obtain R_j^2/F_j^2 versus range for the selected altitudes.
5. Select the altitude where F factor is maximum (R_j is fixed) or altitude and range where R_j^2/F_j^2 is minimum. The optimum altitude and range for the standoff jammer is thus selected. This is an iterative process involving Steps 3, 4, and 5.
6. Calculate SOJ_{fs} from the quantity in brackets in Equation 31. Substitute this value for free-space range in IREPS and generate the standoff burnthrough coverage diagram. The ECM planner uses the standoff burnthrough coverage display to determine the altitude of the attack aircraft to delay burnthrough.
7. The preplanned flight path for the attack aircraft and the standoff altitude and range are completed for a specific radar. The process can be repeated for other situations.

E. PLANNING RESULTS

This section contains sample calculations for determining the optimum location for self-protection and standoff jamming. In both examples, a fictitious low-altitude acquisition-type radar (labled A) will be used along with actual environmental

data from the USS Nimitz. Since IREPS does not calculate the interaction between two directional antennas, the calculation is limited to an omnidirectional jamming antenna. Also, IREPS can only handle the case where the radar uses the same antenna for transmitting and receiving. The self-protection positioning example will consider both a normal, no-duct, and a weak surface-based duct situation. The stand-off example will use only the weak surface-based duct.

1. Self-Protection Noise-Jamming

Step 1. The environmental radar and jammer parameters are simply listed here with no discussion.

A. Environmental Data

1. Normal or "No-duct"

a. Propagation Conditions Summary - Figure 12

b. Environmental Data List - Figure 13

2. Weak Surface-based Duct

a. Propagation Conditions Summary - Figure 9

b. Environmental Data List - Figure 10

B. Radar Data

Name ---------- Radar A

P_t ---------- 1000 KW

G_t ---------- 10,000 (40db)

τ ---------- 2 microseconds

σ ---------- 25 meters^2

(S/N) ---------- 1

L_r ---------- 10 (10db)

Antenna Height ---------- 25 feet

f ---------- 1000 MHZ

Free-Space Range ---------- 80 n.m.

Antenna Type ---------- (Sin X)/X

Vertical Beamwidth -------- 4°

Antenna Elevation Angle --- 1°

C. Jammer Data

P_j - 10 watts/MHZ

G_j - 1 (0 db)

L_j - 1.26 (1 db)

L_p - 2 (3 db)

Step 2. Generate Radar Coverage Displays

The radar A coverage diagrams for the no-duct and weak surface-based duct cases are given in Figures 14 and 11 respectively. The surface-based duct (Figure 11) directs the energy beyond the horizon and "fills in" the area from 40 to 80 nautical miles. The optimum profile for an attack aircraft is not the same for both cases.

For the no-duct case, the standard tactic of flying as low as possible is valid (Figure 15). At an altitude of 500 feet, the aircraft would not be detected until 30 nautical miles (Point A, Figure 15) which agrees closely with the radar horizon of 33.65 nautical miles, using an effective earth's radius of 4/3.

The same attack aircraft at 500 foot altitude could possibly be detected prior to 120 nautical miles when the

weak surface-based duct is present (Point B, Figure 11). By flying slightly above the duct, detection could be delayed until 80 nautical miles (Point C, Figure 16). It can be seen that the surface-based duct has a significant affect on low altitude aircraft detection.

Step 3. Generate Self-Protection Burnthrough Coverage Diagram

Substitution of the radar and jammer parameters into Equation 23 gives a free-space burnthrough range of 15 nautical miles. Figures 17 and 18 are the self-protection burnthrough coverage diagrams for the no-duct and weak surface-based duct cases, respectively. It is important to note that a 15 nautical mile free-space burnthrough range gives an actual burnthrough range of 27 nautical miles at 2000 feet when non-free-space factors are considered (Point D, Figure 17). For the no-duct condition, the attack aircraft should stay at 500 feet or climb to 2400 feet to achieve a burnthrough range of 15 nautical miles. For the weak surface-based duct (Figure 18), the duct eliminates the possibility of penetration at 500 feet (Point E, Figure 18) but 2000 foot penetration is still valid. For penetration at high altitude, radars whose prime function is high altitude coverage would be considered and used to develop the appropriate coverage diagrams.

Step 4. Preplanned Mission

Tactic: Self-protection Noise-jamming

A. Environmental Conditions - "No-Duct"

Penetration Altitude: 500 feet

Probable Detection Range: 30 n.m.

Jammer Initiation Range: 30 n.m.

Burnthrough Altitude: 500 or 2400 feet

Probable Burnthrough Range: 15 n.m.

B. Environmental Conditions - "Weak Surface-Based Duct"

Penetration Altitude: 1200 feet

Probable Detection Range: 80 n.m.

Jammer Initiation Range: 80 n.m.

Burnthrough Altitude: 2000 feet

Probable Burnthrough Range: 15 n.m.

Note: Only one environmental condition would be used for planning each mission.

2. Standoff Noise-Jamming

The example for the standoff noise-jamming will be for a fixed standoff range R_j. The R_j selected was arbitrary but is consistent with the practice of keeping the standoff jammer out of harms way. For the sake of simplicity, only a few F^2 factors will be determined from the path-loss calculation. Therefore, the altitude selected may not be optimum, but illustrates the method of calculation. The determination of the optimum standoff altitude involves running more path-loss diagrams for various altitudes.

A standoff jamming option in IREPS could easily determine the optimum altitude for any standoff jamming range. By selecting the minimum value of R_j^2/F_j^2 for different combinations of range and altitude, the optimum jamming location could be solved quite easily by the computer.

The azimuthal positioning of the standoff jammer was arbitrary selected to give a 6 db reduction in gain (G_{rj} = 34 db) for the jammer-to-radar path. This allowed for gain variations when the jammer aircraft follows a racetrack jamming pattern.

Step 1. Environmental, Radar, and Jammer Parameters

A. Environmental Data

1. Weak Surface-based Duct

a. Propagation Condition Summary - Figure 9

b. Environmental Data List - Figure 10

B. Radar and jammer data are the same as the self-protection example except for P_j = 500 Watts/MHZ and the addition of

G_r ---------- 10,000 (40 db)

G_{rj} ---------- 2512 (34 db)

G_{jr} ---------- 1 (0 db)

R_j ---------- 60 nautical miles.

Step 2. Generate Radar Coverage Display

The radar A coverage diagram for the weak surface-based duct is given in Figure 11. This is the same as was used in the self-protection case. The standoff jammer should

initiate jamming prior to the attack aircraft entering the detection area. Therefore, the initiation of jamming would depend on the altitude of the attack aircraft. As in the self-protection case, the optimum altitude of the attack aircraft is slightly above the duct (Point C, Figure 16).

Step 3. Select Range(s) and Altitude(s)

A standoff range of 60 nautical miles was selected for this example. Probable altitudes of 800, 2000, 4000, 6000, 8000, 10,000, 12,000, and 15,000 feet were selected from the radar A coverage displays.

Step 4. Run Path-Loss Calculation for the Specified Altitudes and Ranges.

Table III is a listing of the F^2 factors for a standoff range of 60 nautical miles and the selected altitudes.

TABLE III

F^2 Values for Various Altitudes
(R_j = 60 nautical miles)

Altitude (ft)	R_j (n.m.)	F^2	R_j^2/F_j^2 (10^3 n.m.^{2})
800	60	1.54	2.32
2000	60	3.01	1.19
4000	60	0.16	21.9
6000	60	2.16	1.66
8000	60	0.29	12.2
10,000	60	0.91	3.64
12,000	60	0.34	10.3
15,000	60	0.11	32.2

As discussed earlier, the minimum value of R_j^2/F_j^2 gives the optimum standoff jamming altitude. For a fixed R_j, the largest value of F^2 is desired. If the range is not fixed, then the value of R_j^2/F_j^2 would change with range. It is therefore possible to compare the jamming effectiveness of flying at the same altitude but at two different ranges.

Step 5. Select Optimum Altitude

The optimum altitude for a standoff range of 60 nautical miles is 2000 feet.

Step 6. Calculate SOJ_{fs} from the quantity in brackets in Equation 31.

Substitution of the radar and jammer parameters, and R_j and F_j into the quantity in brackets in Equation 31 gives a free-space burnthrough range of 13 nautical miles. Figure 19 is the standoff burnthrough coverage diagram for the weak surface-based duct for this burnthrough range. The attack aircraft should penetrate burnthrough at 12 nautical miles flying at an altitude of 1800 feet (Point F, Figure 19). If a lower altitude were selected, the burnthrough range would be closer to 20 nautical miles.

Step 7. Preplanned Mission

Tactic: Standoff Noise-Jamming

Environmental Conditions: "Weak Surface-Based Duct"

Penetration Altitude: 1200 feet

Probable Detection Range: 80 n.m.

Jammer Initiation Range: 80 n.m.

Burnthrough Altitude: 1800 feet

Probable Burnthrough Range: 12 n.m.

Standoff Range: 60 n.m.

Standoff Altitude: 2000 feet

IREPS REV 2.0

**** PROPAGATION CONDITIONS SUMMARY ****

LOCATION: NIMITZ
DATE/TIME: 0014Z 11 FEB 80 (N)

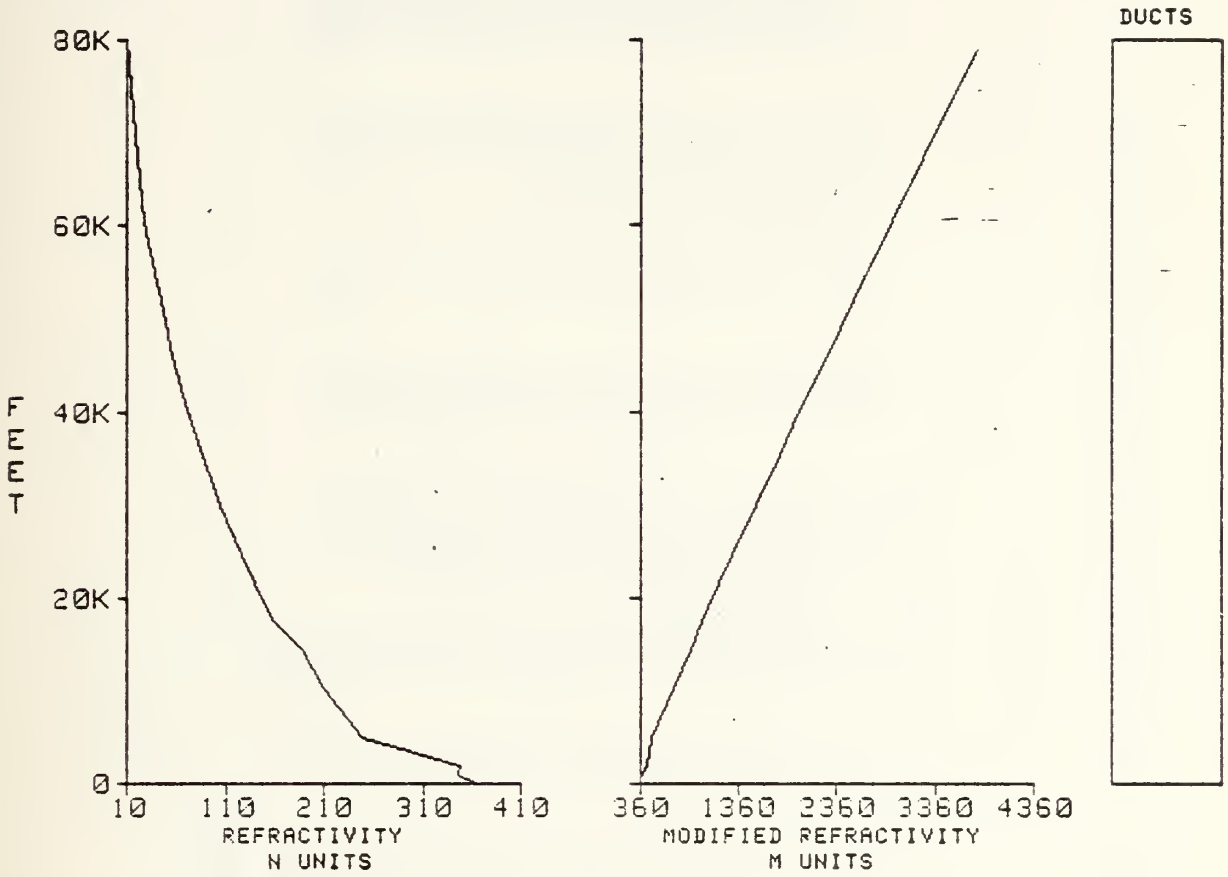

WIND SPEED= 8.0 KNOTS

SURFACE-TO-SURFACE
NORMAL RANGES AT ALL FREQUENCIES

SURFACE-TO-AIR
NORMAL RANGES AT ALL ALTITUDES.

AIR-TO-AIR
NORMAL RANGES AT ALL ALTITUDES.

SURFACE REFRACTIVITY: 366 --SET SPS-48 TO 377

Figure 12. Propagation Conditions Summary for No-Duct

IREPS REV 2.0

**** ENVIRONMENTAL DATA LIST ****

LOCATION: NIMITZ
DATE/TIME: 0014Z 11 FEB 80 (N)

WIND SPEED 8.0 KNOTS SURFACE PRESSURE = 1012.9 mB
RADIOSONDE LAUNCH HEIGHT = 32.8 FEET

LEVEL	PRESS (mB)	TEMP (C)	RH (%)	DEW PT DEP(C)	FEET	N UNITS	N/Kft	M UNITS	CONDITION
1	1,012.9	22.4	86.0	2.4	32.8	365.7	-28.1	367.3	SUPER
2	1,000.0	20.8	86.0	2.4	399.0	355.4	-15.9	374.5	NORMAL
3	978.0	18.5	91.0	1.5	1,029.9	345.4	4.2	394.6	SUB
4	951.0	22.5	85.0	2.6	1,826.7	348.7	-31.6	436.1	SUPER
5	850.0	16.3	25.0	20.2	5,001.7	248.5	-7.5	487.8	NORMAL
6	700.0	5.7	32.0	15.6	10,313.2	208.8	-5.3	702.2	NORMAL
7	600.0	-3.0	60.0	6.7	14,386.6	187.3	-9.4	875.6	NORMAL
8	533.0	-6.0	19.0	30.0	17,447.3	158.7	-4.9	993.4	NORMAL
9	500.0	-11.1	19.0	30.0	19,073.3	150.7	-4.6	1,063.2	NORMAL
10	400.0	-24.0	19.0	30.0	24,555.9	125.6	-3.9	1,300.4	NORMAL
11	318.0	-36.4	19.0	30.0	29,912.9	104.6	-3.4	1,535.6	NORMAL
12	300.0	-39.1	45.0	7.4	31,231.2	100.1	-3.6	1,594.2	NORMAL
13	250.0	-45.7	19.0	30.0	35,274.6	85.4	-3.0	1,773.0	NORMAL
14	200.0	-54.4	19.0	30.0	40,059.1	71.0	-2.6	1,987.5	NORMAL
15	150.0	-64.0	19.0	30.0	45,974.4	55.7	-2.0	2,255.2	NORMAL
16	110.0	-76.3	19.0	30.0	52,025.6	43.3	-2.1	2,532.3	NORMAL
17	100.0	-76.6	19.0	30.0	53,827.1	39.5	-1.8	2,614.7	NORMAL
18	70.0	-71.1	19.0	30.0	60,659.1	26.9	-1.2	2,928.9	NORMAL
19	50.0	-67.5	19.0	30.0	67,251.0	18.9	-.8	3,236.3	NORMAL
20	30.0	-63.8	19.0	30.0	77,438.0	11.1	-.6	3,715.9	NORMAL
21	28.0	-60.5	19.0	30.0	78,837.3	10.2	------	3,782.0	------

SURFACE REFRACTIVITY: 366 --SET SPS-48 TO 377

Figure 13. Environmental Data List for No-Duct

IREPS REV 2.0

**** COVERAGE DISPLAY ****

RADAR A EL 1

LOCATION: NIMITZ
DATE/TIME: 0014Z 11 FEB 80 (N)

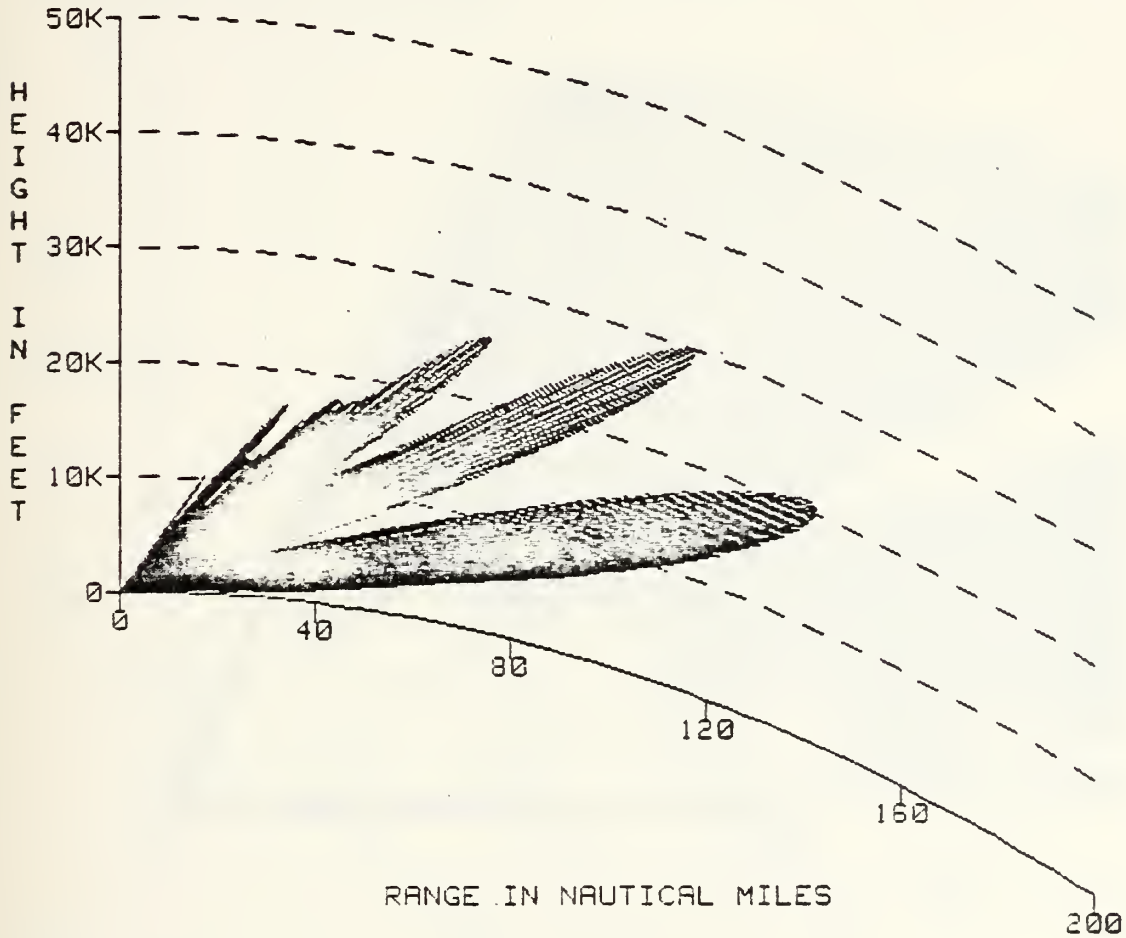

RADAR A
EL 1 BEAMWIDTH 4

SHADED AREA INDICATES AREA OF DETECTION OR COMMUNICATION

FREE SPACE RANGE: 80.0 NAUTICAL MILES
FREQUENCY: 1000 MHZ
TRANSMITTER OR RADAR ANTENNA HEIGHT: 25.0 FEET

Figure 14. 200 Nautical Mile Radar A Coverage Diagram for No-Duct

IREPS REV 2.0

**** COVERAGE DISPLAY ****

RADAR A EL 1

LOCATION: NIMITZ
DATE/TIME: 0014Z 11 FEB 80 (N)

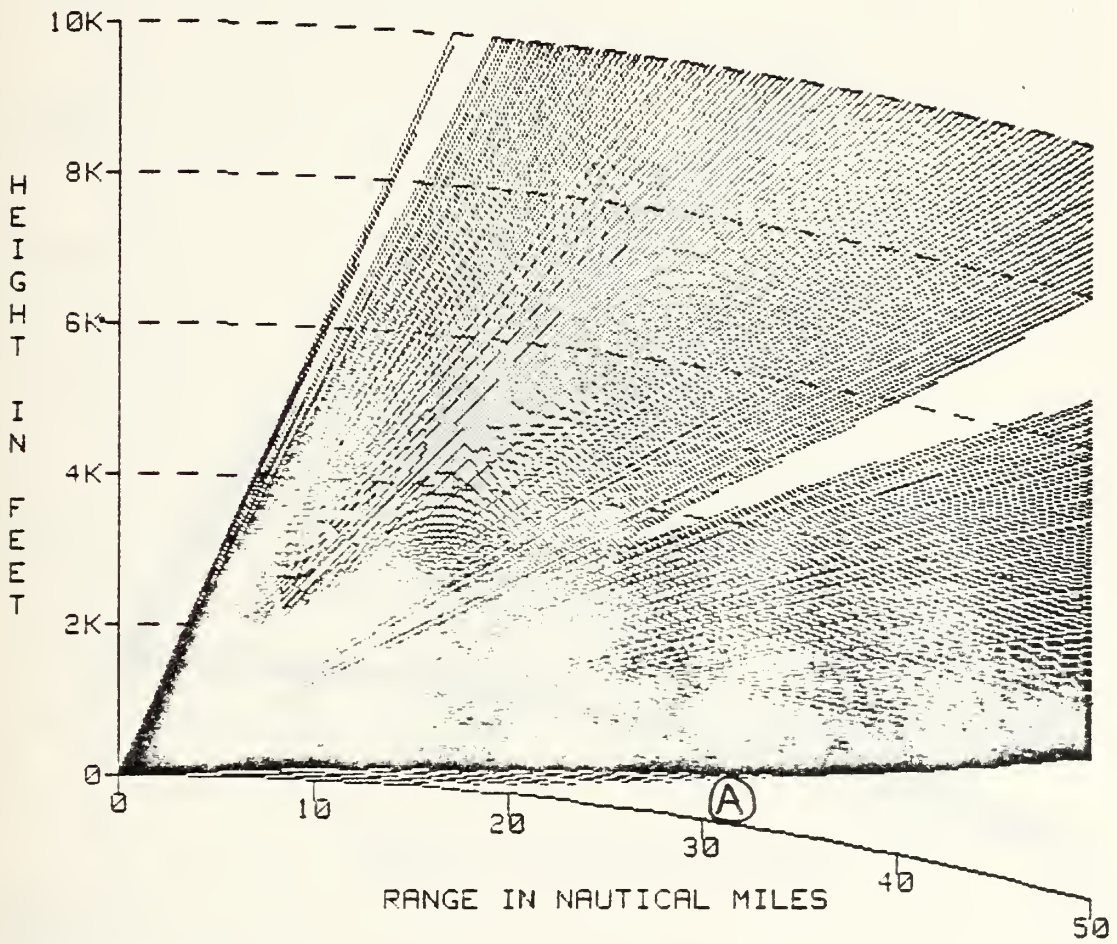

RADAR A
EL 1 BEAMWIDTH 4

SHADED AREA INDICATES AREA OF DETECTION OR COMMUNICATION

FREE SPACE RANGE: 80.0 NAUTICAL MILES
FREQUENCY: 1000 MHZ
TRANSMITTER OR RADAR ANTENNA HEIGHT: 25.0 FEET

Figure 15. 50 Nautical Mile Radar A Coverage Diagram for No-Duct

IREPS REV 2.0

**** COVERAGE DISPLAY ****

RADAR A EL 1

LOCATION: NIMITZ
DATE/TIME: 2333Z 8 FEB 80 (N)

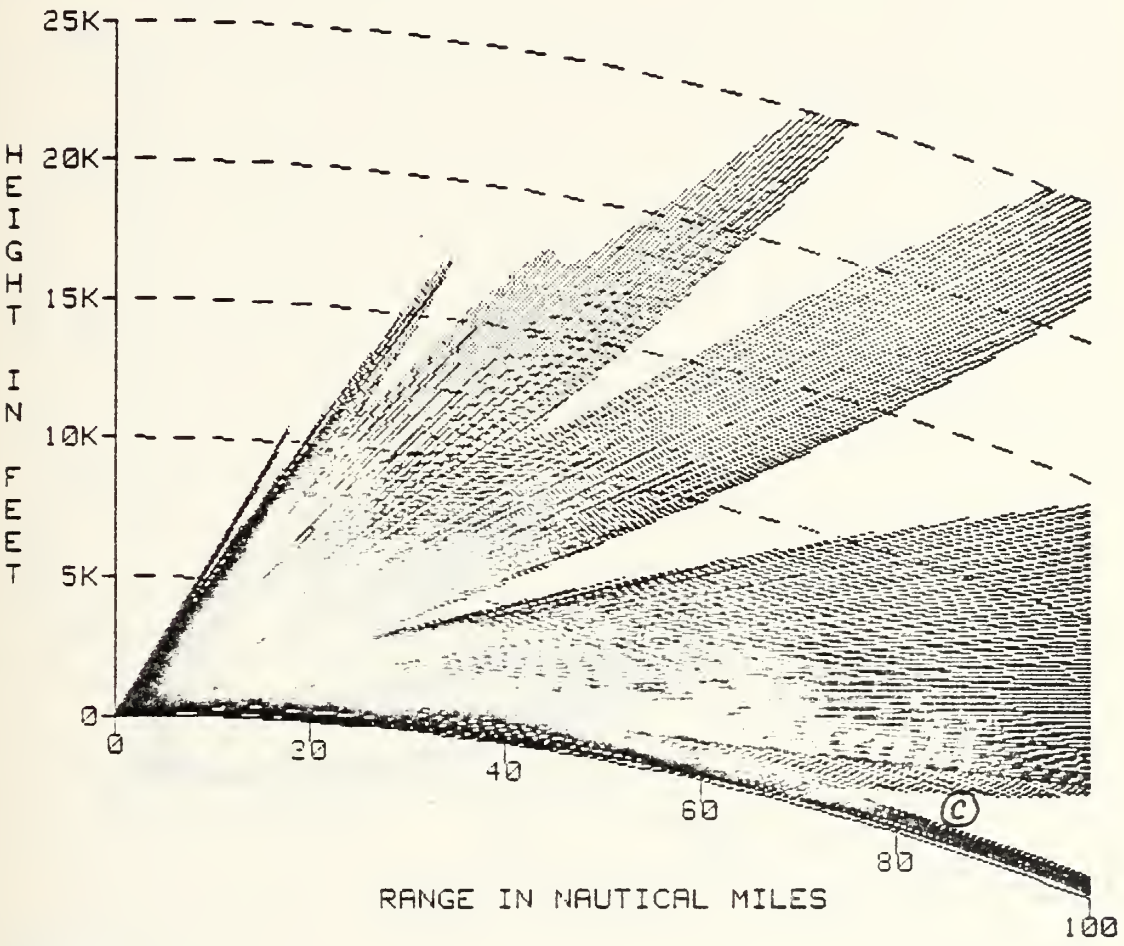

RADAR A
EL 1 BEAMWIDTH 4

SHADED AREA INDICATES AREA OF DETECTION OR COMMUNICATION

FREE SPACE RANGE: 80.0 NAUTICAL MILES
FREQUENCY: 1000 MHZ
TRANSMITTER OR RADAR ANTENNA HEIGHT: 25.0 FEET

Figure 16. 100 Nautical Mile Radar A Coverage Diagram for a Weak Surface-Based Duct

IREPS REV 2.0

**** COVERAGE DISPLAY ****

RADAR A EL 1 SPR

LOCATION: NIMITZ
DATE/TIME: 0014Z 11 FEB 80 (N)

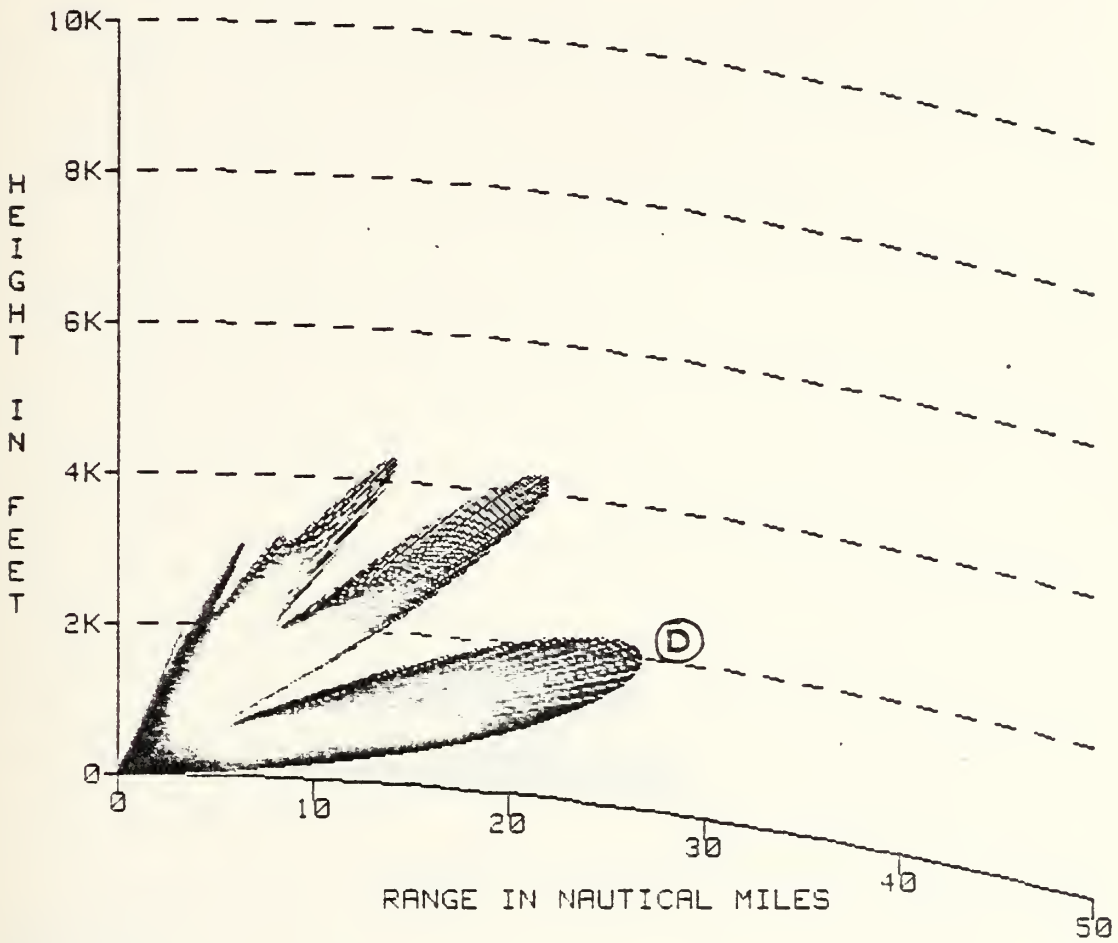

RADAR A SPR
EL 1 BEAMWIDTH 4 FSR 15

SHADED AREA INDICATES AREA OF DETECTION OR COMMUNICATION

FREE SPACE RANGE: 15.0 NAUTICAL MILES
FREQUENCY: 1000 MHZ
TRANSMITTER OR RADAR ANTENNA HEIGHT: 25.0 FEET

Figure 17. Self-Protection Burnthrough Coverage Diagram for No-Duct

IREPS REV 2.0

**** COVERAGE DISPLAY ****

RADAR A EL 1 SPR

LOCATION: NIMITZ
DATE/TIME: 23332 8 FEB 80 (N)

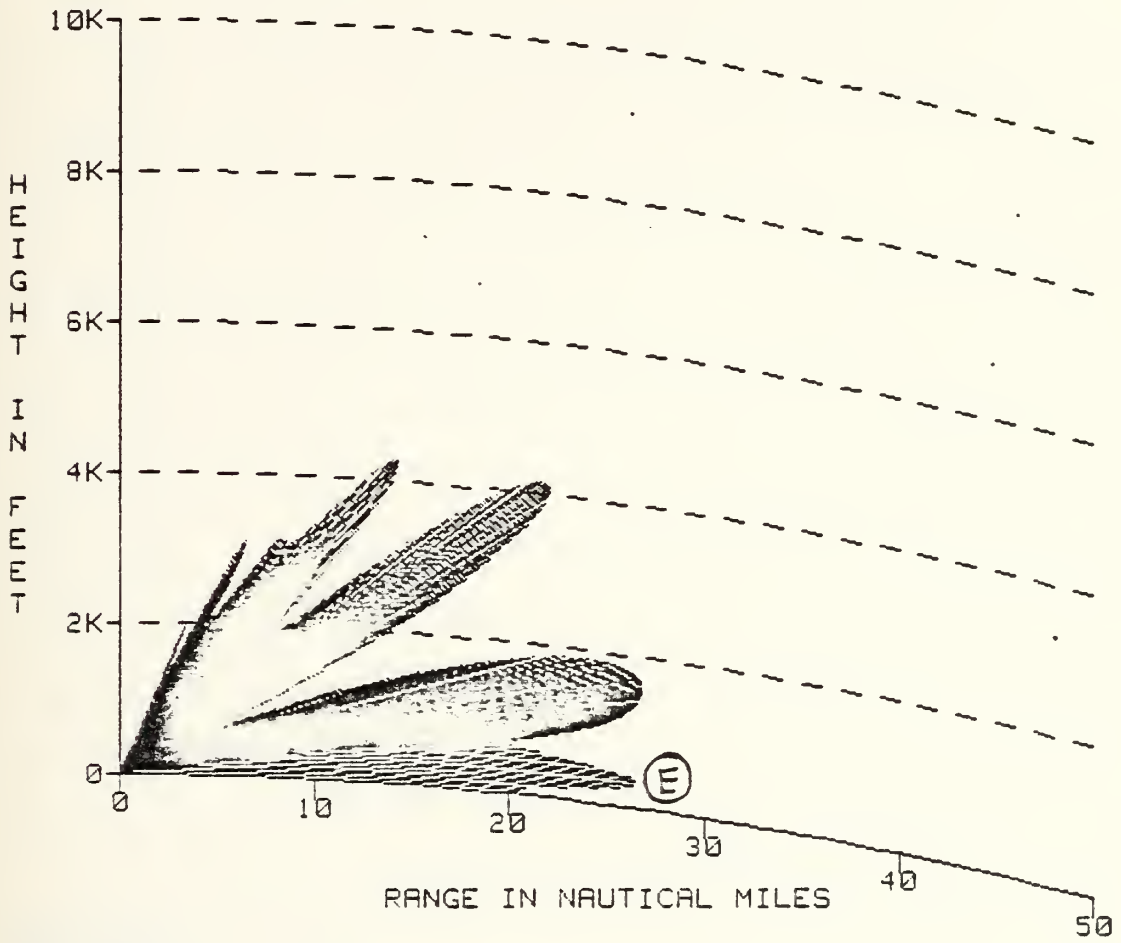

RADAR A SPR
EL 1 BEAMWIDTH 4 FSR 15

SHADED AREA INDICATES AREA OF DETECTION OR COMMUNICATION

FREE SPACE RANGE: 15.0 NAUTICAL MILES
FREQUENCY: 1000 MHZ
TRANSMITTER OR RADAR ANTENNA HEIGHT: 25.0 FEET

Figure 18. Self-Protection Burnthrough Coverage Diagram for a Weak Surface-Based Duct

IREPS REV 2.0

**** COVERAGE DISPLAY ****

RADAR 1 EL 1 SOJ

LOCATION: NIMITZ
DATE/TIME: 2333Z 8 FEB 80 (N)

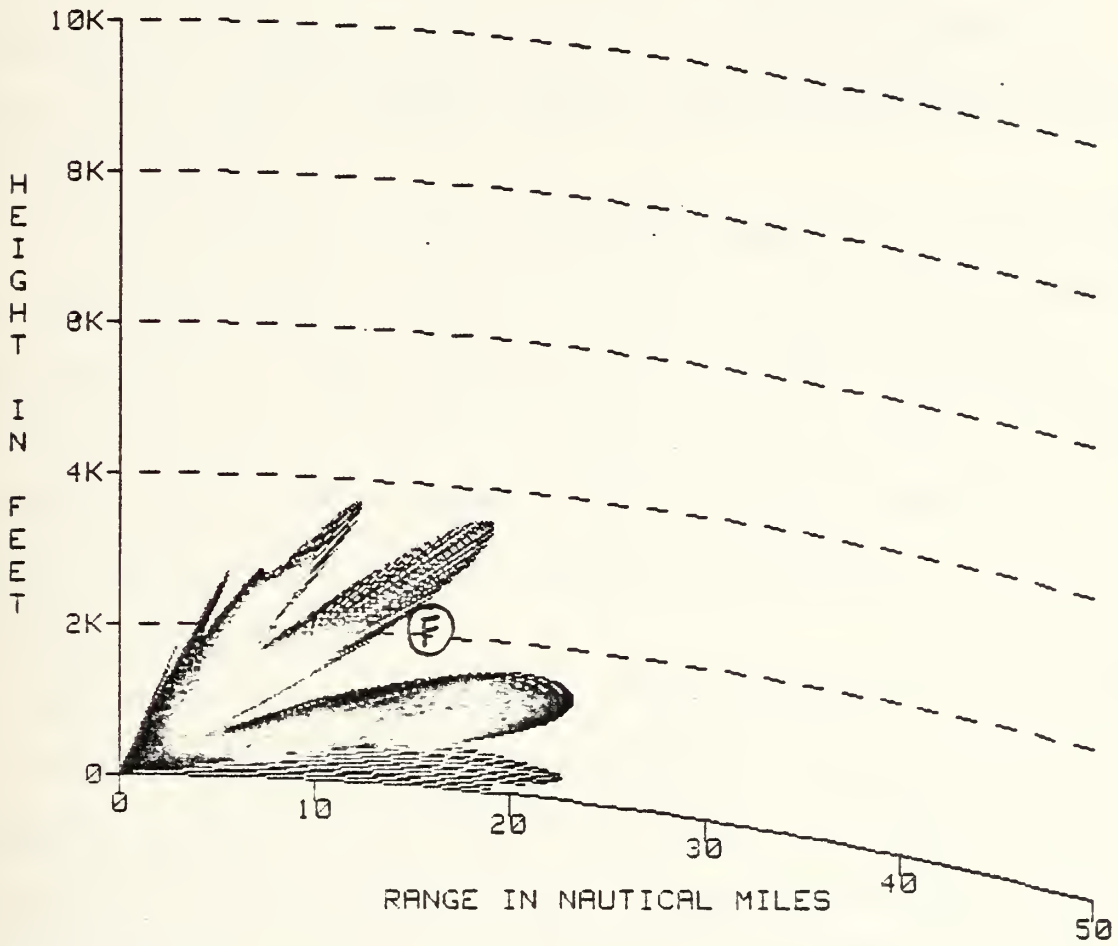

RADAR A SOJ
EL 1 BEAMWIDTH 4 FSR 13

SHADED AREA INDICATES AREA OF DETECTION OR COMMUNICATION

FREE SPACE RANGE: 13.0 NAUTICAL MILES
FREQUENCY: 1000 MHZ
TRANSMITTER OR RADAR ANTENNA HEIGHT: 25.0 FEET

Figure 19. Standoff Burnthrough Coverage Diagram for a Weak Surface-Based Duct

VI. CONCLUSIONS AND RECOMMENDATIONS

Advances in computer technology and the modeling of environmental effects can give the ECM planner the tools to optimize both the horizontal and vertical positioning of active ECM assets. The ability to measure the atmospheric conditions and apply those results in the development of tactics can lead to optimum jamming effectiveness and reduced aircraft losses.

The Integrated Refractive Effects Prediction System (IREPS) has the capability to make the needed calculations for optimum positioning. The implementation of IREPS, including a jamming package, will give the ECM planner a "true" tactical planning aid. In this sense, "true" tactical planning is when consideration is given to both the warfare situation and the environment.

IREPS was designed to aid in the assessment of the impact of lower atmospheric refractive effects on naval electromagnetic systems. With minor modifications, IREPS, as it exists, can provide valuable ECM planning information. However, the development of an ECM option in IREPS would provide a much improved capability.

IREPS is currently limited to the maritime environment. The overland case is of interest to both the U.S. Air Force and U.S. Navy. To apply an IREPS type model for overland terrain, the reflection coefficient and changes in refraction

conditions with location must be known. The examples in this thesis are applicable to both the U.S. Air Force fighter and bomber aircraft that penetrate a coastal region as well as the naval aircraft in the pure open-ocean environment. Since the threat and environmental conditions are the same for the U.S. Air Force and U.S. Navy, a joint effort to develop an ECM option would be beneficial to both.

The development of a specific ECM option could eliminate many of the current IREPS limitations. IREPS, as it is now, handles the omnidirectional jamming antenna case but programming work is required for the directional jamming antenna. At the present time, the ECM planner can solve the free-space jamming equations, by whatever means, and run burnthrough coverage diagrams using that information. The planner must interpret the output information. However, if an ECM option were developed to be interactive with the ECM planner (the current IREPS is extremely user friendly), detection information could be provided from the radar coverage diagrams, the free-space jamming equations could be solved automatically and the burnthrough coverage diagrams automatically displayed. The ECM planner could determine optimum attack altitudes with minimal technical knowledge of environmental and electromagnetic effects. More time would be available from planning rather than concern about technical details or solutions of jamming equations. Validated hostile radar and jamming system data bases could be provided in the ECM option. A more systems approach to the problem could then be realized.

The use of IREPS for positioning jamming aircraft is available now. With the proper data tapes to compute the free-space burnthrough equations and modified path-loss calculations for determining F factors, a jamming version of IREPS could be available to selected Air Force and Navy users. The feedback received from such use would provide operational considerations in the development of an automated ECM option for IREPS.

APPENDIX A

EXCERPTS FROM IREPS USER'S MANUAL

The following are excerpts from the IREPS User's Manual. The different IREPS products and tactical uses of IREPS are discussed. For more information on IREPS, contact:

Naval Ocean System Center
Attn: H.V. Hitney, Code 5325
San Diego, California 92152

1.0. INTRODUCTION

1.1. Purpose

The purpose of this manual is to introduce the reader to a variety of effects that the lower atmosphere (troposphere) can have on the performance of many naval electromagnetic (EM) systems and to describe the Interim Integrated Refractive Effects Prediction System (IREPS) as implemented on the Hewlett-Packard model 9845 desktop calculator. Atmospheric refraction affects radar, UHF and microwave communications, and electronic warfare and missile guidance systems. The effects described in this document are important only at EM frequencies above 100 MHZ. Upper atmosphere (ionosphere) effects on HF communications or other systems are <u>not</u> discussed.

1.2. The IREPS Concept

IREPS is a shipboard environmental data processing and display system designed to aid in the assessment of the impact of lower atmospheric refractive effects on naval EM systems. In its final form IREPS will be implemented using fully militarized hardware and software which may be combined with the shipboard version of the Naval Environmental Display Station (NEDS II) to form a Shipboard Environmental Support Center (SESC). Since a final configuration may not be realized for several years, an Interim version of IREPS has been developed for implementation aboard CV/CVNs using a Hewlett-Packard desktop calculator (HP 9845).

IREPS has been developed, and is continuing to be refined at Naval Ocean Systems Center (NOSC), to give a comprehensive refractive effects assessment capability for naval surveillance, communications, electronic warfare, and weapons guidance systems. IREPS has been successfully used under operational conditions aboard selected CV/CVNs to assess and exploit refractive effects in tactical situations. The Interim IREPS unit should give each CV/CVN a capability that has never before existed and provide the opportunity for early interaction between laboratory and operations personnel to further define and expedite development of refractive effects assessment capabilities.

Prior to describing the operation of the Interim IREPS a background description of the causes and potential impacts of atmospheric refractive effects on naval EM systems is presented (Section 2.0).

2.0 BACKGROUND

2.1 WHAT ARE REFRACTIVE EFFECTS?

The term "refractive effects" refers to the property of a medium (here, the lower atmosphere) to refract or bend an EM wave as it passes through the medium. In this document, the term is taken to imply a wider meaning which includes all propagation effects of, or related to, the lower atmosphere that affect the performance of EM systems. As such, the term includes not only refraction and ducting, but also reflection from the sea surface, multipath interference, diffraction around the earth's surface, tropospheric scattering, sea clutter, and many other propagation mechanisms or processes. For most naval EM systems, the occurrence of ducting in the troposphere provides the most dramatic impact on system performance.

2.1.1 Ducting and Refraction

The term "ducting," as used in this document, means the concentration of radio (or radar) waves in the lowest part of the troposphere in regions characterized by rapid vertical changes in air temperature and/or humidity. Such atmospheric ducts are very analogous to the ducts encountered in ocean acoustic propagation resulting from vertical changes in pressure, temperature, and salinity in the ocean. "Surface ducting" means such concentration of radar waves immediately adjacent to the sea surface. To understand these concepts, a knowledge of the bending, or refraction, of radar waves in the atmosphere will be required. The refractive index, n, of a parcel of air is defined as the ratio of the velocity of propagation of an electromagnetic (e.g. radar) wave in vacuum to that in the air. Since electromagnetic waves travel slightly slower in air than in a vacuum, the refractive index is slightly greater than unity. At the earth's surface, the numeric value of the refractive index n is usually between 1.000250 and 1.000400. In order to have a number that is easier to handle, the refractivity N has been defined to be $N = (n - 1) \times 10^6$, such that surface values of refractivity N vary between 250 and 400. Refractivity can be expressed as a function of atmospheric pressure, temperature, and humidity by the relation:

$$N = \frac{77.6P}{T} + \frac{3.73 \times 10^5 e}{T^2}, \qquad (1)$$

where

P is atmospheric pressure in millibars,

T is temperature in Kelvins, and

e is water vapor pressure in millibars.

For a well-mixed "standard" atmosphere, both temperature and humidity decrease with altitude, such that N decreases with height at a rate of about 39 N units per 1000 metres (or 12 N units per 1000 ft). The behavior of an EM wave propagating horizontal to the earth's surface is such that it will bend or "refract" toward the region of higher refractivity (lower velocity). For the standard atmosphere, a radar wave will bend down toward the earth's surface, but with a curvature less than the earth's, as illustrated in figure 1. If, however, the air temperature increases with altitude or the humidity decreases abnormally fast with altitude, then N will decrease with height much faster than normal. If N decreases

faster than 157 N units per 1000 metres (48 N units per 1000 ft), then a radar wave will refract downwards with a curvature exceeding the earth's curvature and a surface duct will be formed, as illustrated by the example in figure 2. Note that, while the radar wave refracts towards the sea surface, it reflects or "bounces" upward from the sea in this example. It is the continuous refracting down and reflecting up that forms the surface duct and allows for surface detections far beyond the normal horizon.

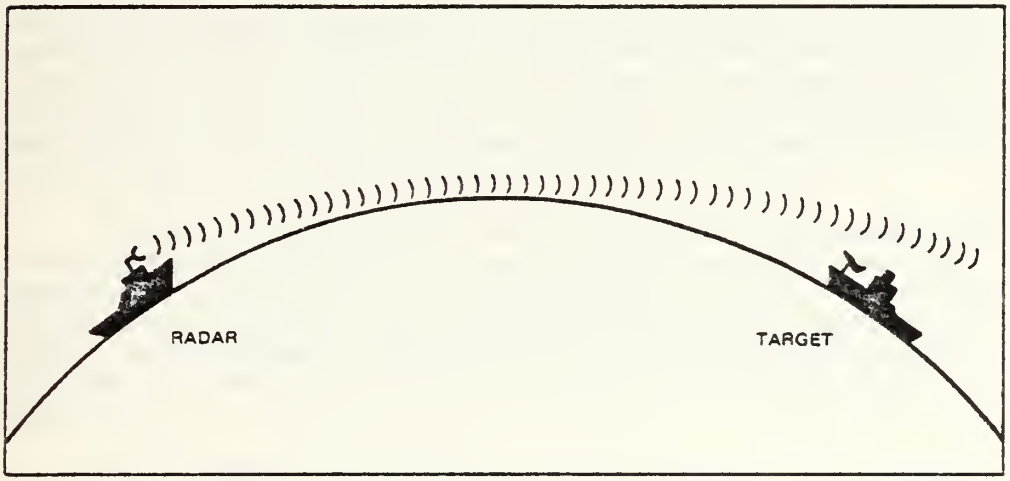

Figure 1. Radar wave path under "standard" atmospheric conditions. Note path curves downward but at a rate less than the earth's curvature. Beyond-the-horizon target detection is not possible.

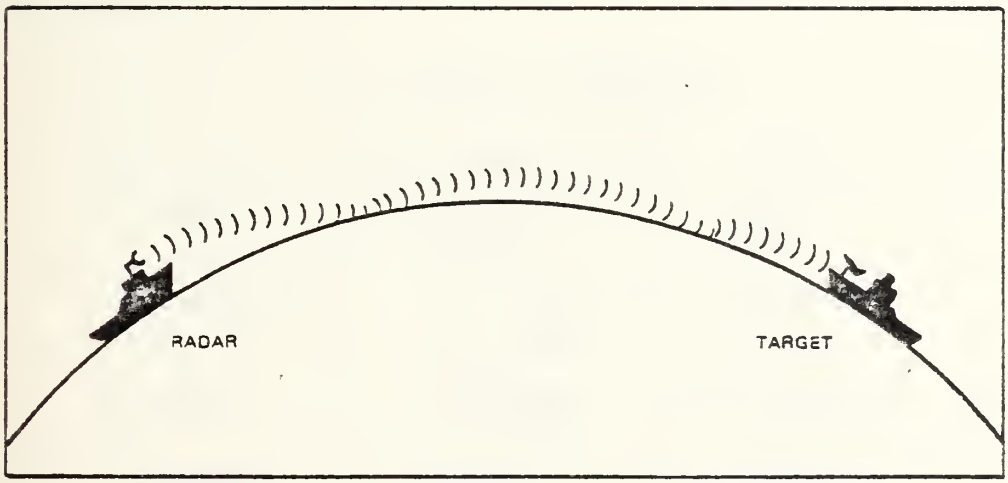

Figure 2. Radar wave path under ducting conditions. Path curves downward at a rate exceeding the earth's curvature resulting in beyond-the-horizon target detection.

As a convenience in determining the occurrence of ducting, the modified refractivity M has been developed. M is related to N by

$$M = N + 0.157\,h \text{ for altitude } h \text{ in metres, or} \qquad (2)$$

$$M = N + 0.048\,h \text{ for altitude } h \text{ in feet.}$$

The modified refractivity takes into account the curvature of the earth in such a way that the presence of ducting can be determined from a simple inspection of M plotted versus height. Whenever M decreases with height, a so-called trapping layer is formed wherein an EM wave can be refracted towards the earth's surface, thus forming a duct. Figure 3 shows N and M plotted versus height for a standard atmosphere, and figure 4 shows N and M plotted versus height for one type of surface ducting condition, illustrating the concept.

In figure 3, M constantly increases with height; hence, there is no trapping layer or resulting duct formed. In figure 4, M decreases with height in one region and thus forms a trapping layer. If the M value at the top of the trapping layer is less than the M value at the surface, then a surface-based duct will be formed in the height interval indicated by the dashed vertical line in figure 4. If the M value at the top of the trapping layer is greater than the M value at the surface, then a so-called elevated duct will be formed as indicated in figure 5.

Besides trapping, there are three other terms that describe the vertical gradient or change with height of N and M: namely superrefractive, standard, and subrefractive. Superrefractive implies an N gradient that is stronger than the normally expected or standard gradient, but *not strong enough to form trapping.* Subrefractive implies an N-gradient weaker than the standard gradient which results in less refraction or bending than normal. Figure 6 graphically shows the relative amounts of bending for each of the four types of refraction. Table 1 shows the definition of these four types of refraction in terms of the N- and M-gradients.

Table 1. Relation of N- and M-gradients

	N-Gradient	M-Gradient
Trapping	≤ -157 N/km	≤ 0 M/km
	≤ -48 N/kft	≤ 0 M/kft
Superrefractive	-157 to -79 N/km	0 to 79 M/km
	-48 to -24 N/kft	0 to 24 M/kft
Standard	-79 to 0 N/km	79 to 157 M/km
	-24 to 0 N/kft	24 to 48 M/kft
Subrefractive	> 0 N/km	> 157 M/km
	> 0 N/kft	> 48 M/kft

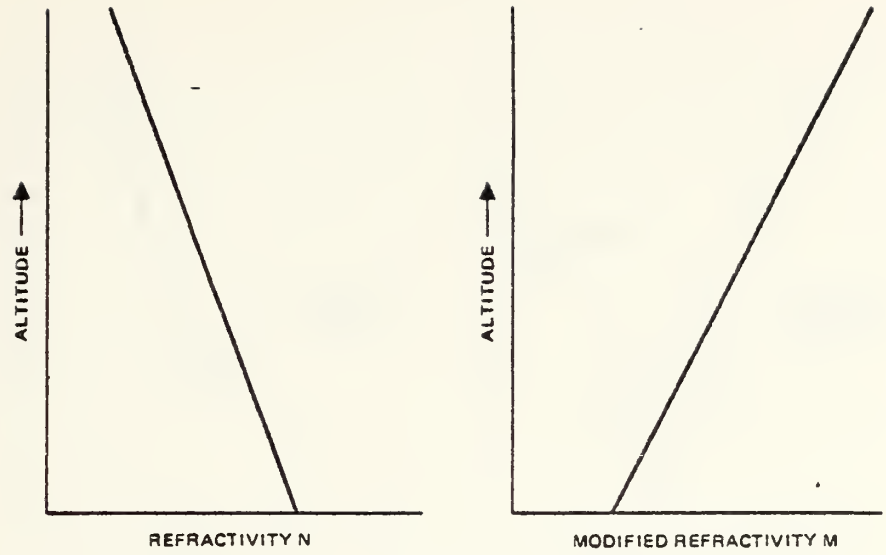

Figure 3. Refractivity N and modified refractivity M versus altitude for a standard atmosphere.

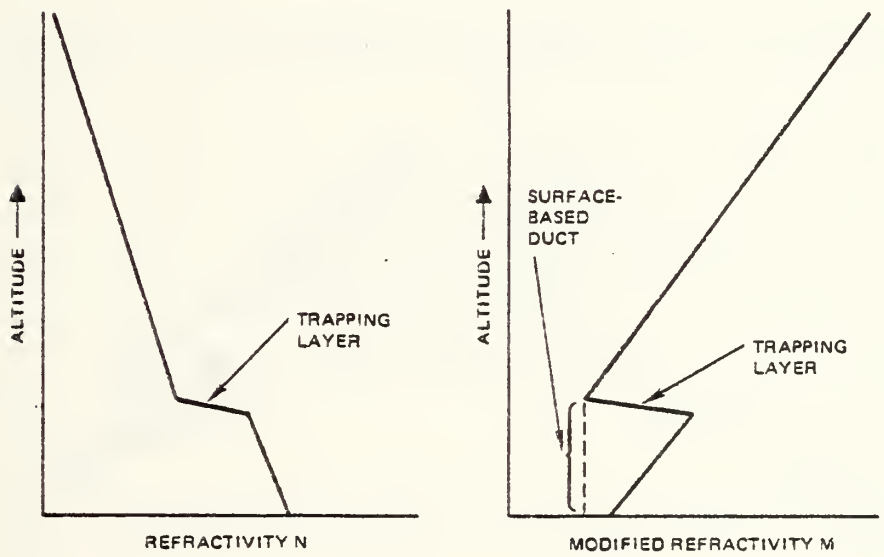

Figure 4. Refractivity N and modified refractivity M versus altitude for a surface-based duct created by an elevated trapping layer.

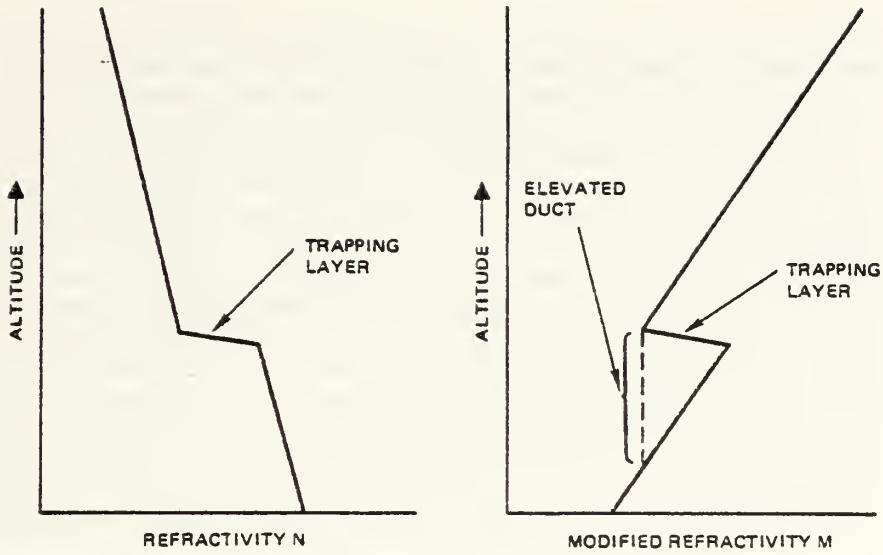

Figure 5. Refractivity N and modified refractivity M versus altitude for an elevated duct created by an elevated trapping layer.

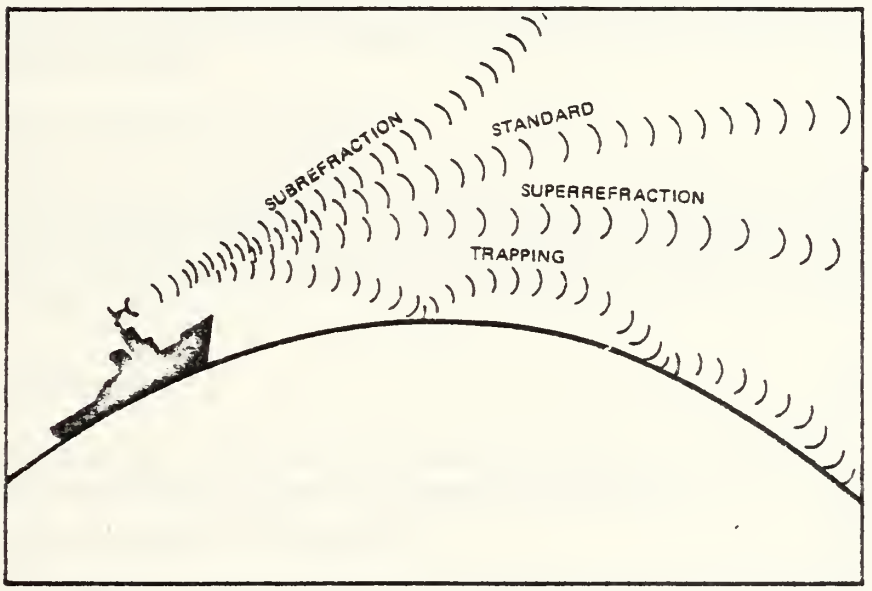

Figure 6. Relative bending for the four types of refraction.

2.1.2 Types of Ducts

There are three distinct types of ducts that are of concern to naval EM systems and each must be treated separately. The three types are: (1) surface-based ducts from elevated refractive layers, (2) elevated ducts, and (3) evaporation ducts. Surface-based ducts from elevated refractive layers generally give extended detection, intercept, and communication ranges for all frequencies above 100 MHz, provided both the transmitter and receiver (or radar and target) are near to or within the duct. Such surface-based ducts are nearly always less than 1 km (3000 ft) thick, although thicknesses of up to 300 m (1000 ft) are more common. Elevated ducts primarily affect air-to-air surveillance, communication, EW, or weapons guidance systems. For instance, detection ranges of air targets by airborne early warning radars can be greatly extended if both the radar and target are in an elevated duct; but at the same time, radar "holes" or blind spots can occur for radars or targets above the duct. Elevated ducts occur at altitudes of near zero to 6 km (20 000 ft), although maximum altitudes of 3 km (10 000 ft) are far more common. The evaporation duct is created by the very rapid decrease of moisture at the air/sea interface and, although variable in its strength, most frequently extends ranges for surface-to-surface systems operating above 3 GHz. Each of these three types of ducts will be discussed in more detail in later sections of this document; but first, an introduction to standard (non-ducting) propagation mechanisms will be presented.

2.2 STANDARD PROPAGATION MECHANISMS

Standard propagation mechanisms are those propagation mechanisms and processes that are, in effect, independent of the existing refractivity conditions. Although standard propagation mechanisms are often described in terms of a standard refractivity profile that has a linear decrease of refractivity of about 12 N units per thousand feet, the mechanisms are generally present for all refractivity conditions even though they may be dominated by the various types of ducting.

2.2.1 Path Loss and Free Space Propagation

If an EM wave is propagating from a transmitter to a receiver (or target) and both the transmitter and receiver are sufficiently far removed from the earth or other objects, the EM wave is said to be propagating in free space. Let P_t be the power transmitted and P_r be the power received. Then the path loss (or propagation loss) between the transmitter and receiver, in decibles, is defined to be

$$L = 10 \operatorname{Log}_{10} \frac{P_t}{P_r} \text{ dB.} \tag{3}$$

In free space, the path loss is determined by the geometrical spreading of the power over the surface of the expanding sphere centered at the transmitter and is given by

$$L_{fs} = 37.8 + 20 \operatorname{Log}_{10} f + 20 \operatorname{Log}_{10} R \text{ dB;} \tag{4}$$

where, f is the transmitter frequency in MHz and R is the range between the transmitter and receiver in nmi. Equation (4) assumes that both the transmitter and receiver employ lossless isotropic (radiating uniformily in all directions) antennas. L_{fs} would be a good approximation for path loss between two aircraft, if both aircraft were at reasonably high altitudes and

there were no elevated ducts present near their altitudes. However, for a transmitter or receiver near the surface, reflections from the surface must be taken into account.

2.2.2 Reflection and the Interference Region

When an EM wave strikes a nearly smooth large surface, such as the ocean, a portion of the energy is reflected from the surface and continues propagating along a path, which makes an angle with the surface equal to that of the incident ray, as illustrated by figure 7. The strength of the reflected wave is determined by the reflection coefficient which depends upon the frequency and polarization of radiation, the angle of incidence, and the roughness of the reflecting surface disturbed by the wind. Not only is the magnitude of the reflected wave reduced, but the phase of the EM wave is also altered. Typical values for the reflection coefficient for shallow incidence angles and smooth seas are .99 (i.e., the reflected wave is 99 percent as strong as the incidence wave) and 180 degrees of phase change.

As the wind speed increases, the ocean surface grows rougher and the reflection coefficient can decrease to about .15 (the phase change is unaffected). For a transmitter near the surface, the reflection process results in two paths to a receiver (or target) within line-of-sight, as illustrated by figure 8. As the geometry changes in figure 8, the relative lengths of the direct path and reflected path also change, which results in the direct and reflected wave arriving at the receiver in varying amounts of phase difference. The received signal strength is the vector sum of the signal strengths of the direct and reflected wave, which causes the received power to vary up to 6 dB above and up to 20 dB or more below the free space value.

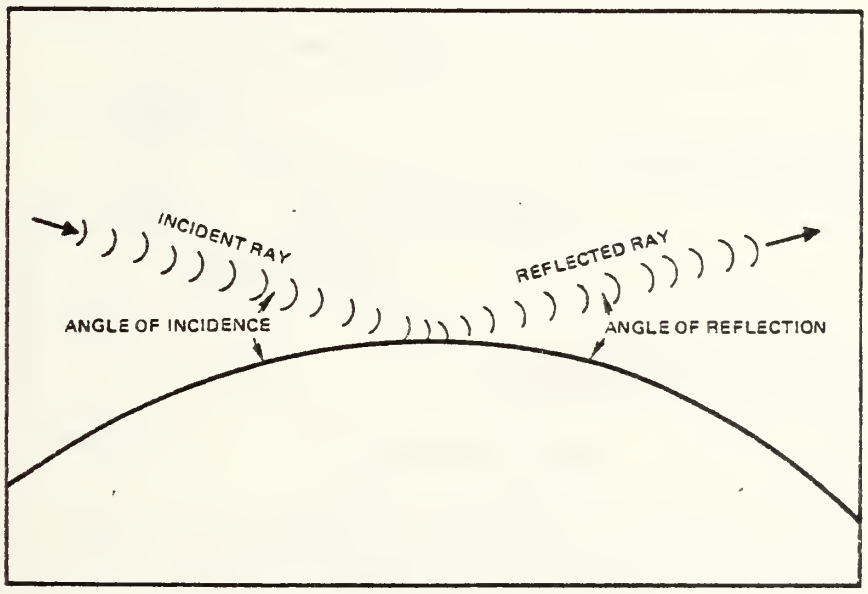

Figure 7. Incident ray and reflected ray illustrating equal angles of reflection.

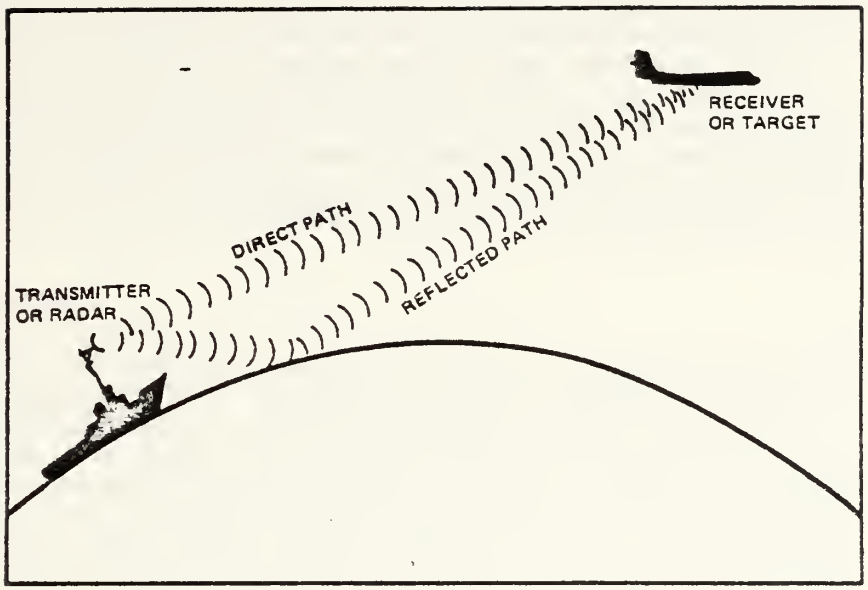

Figure 8. Surface-to-air geometry illustrating direct and sea-reflected paths.

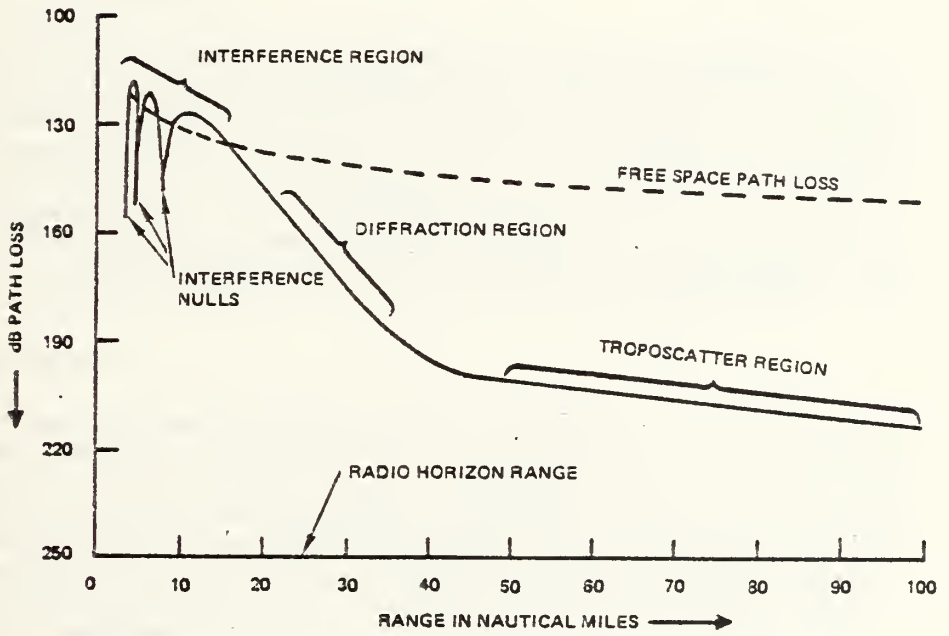

Figure 9. Path loss curve for a 5000 MHz transmitter at 60 ft and a receiver at 100 ft for a standard atmosphere.

Figure 9 shows a plot of path loss versus range for a 5000 MHz (5 GHz) transmitter located 60 ft above the sea surface and a receiver at 100 ft above the sea surface for standard refractive conditions. The region in which the path loss is dominated by the interference of the direct and sea-reflected wave is called the interference region and is labeled as such in figure 9. The free space path loss, as calculated from equation (4), is included in figure 9 for reference and illustrates how the path loss oscillates above and below the free space value in the interference region. The depth of the nulls depends very much on the surface roughness related to the wind speed. The example here, is for a smooth sea surface associated with zero wind speed, but as the wind speed increases the path loss in the nulls would approach the free space value.

2.2.3 Diffraction

Near the radio horizon range, where the path between the transmitter and receiver is just tangent to the earth's surface, the path loss is dominated by diffraction around the earth. The diffraction region, which is sometimes called the shadow region, is characterized by propagation beyond the line of sight or radio horizon because of the ability of a radio wave to travel along an interface of dissimilar materials, in this case, the earth's surface and the atmosphere. The amount of power, or signal strength, available to a receiver in this region is very dependent on the refractive conditions near the earth's surface. In fact, the various forms of ducting to be described in the following sections are actually special cases of propagation in the diffraction region. To calculate path loss in the diffraction region, in any case, is very complicated and is usually based on notions of normal-mode propagation and atmospheric waveguide considerations.

2.2.4 Tropospheric Scatter

At ranges far beyond the horizon, the path loss is dominated by a mechanism called tropospheric scatter or troposcatter (fig 9). Propagation in the troposcatter region is the result of scattering of the EM wave from refractive heterogeneities at relatively high altitudes, that are line-of-sight to both the transmitter and receiver. The calculation of path loss in the troposcatter region is quite easily performed using semi-empirical formulations. The rate at which the path loss increases with range, within the troposcatter region, is considerably less than the rate in the diffraction region (fig 9). However, the path loss values found in this region are so high that it is impossible for any known radar system to detect targets. Troposcatter is an important consideration for certain communications systems and ESM receivers.

2.2.5 Absorption

A standard propagation mechanism that was not illustrated in figure 9, but should be mentioned, is absorption. Oxygen and water vapor molecules in the atmosphere absorb some energy from radio waves and convert it to heat. The amount of absorption is highly dependent on the radio frequency and is negligible, compared to all the other propagation considerations, below 20 GHz. Also, absorption by rain drops and other forms of precipitation can be important at some frequencies, but this type of absorption is very hard to model and even harder to acquire environmental data on. For these reasons, absorption effects are ignored in the IREPS programs.

2.2.6 Maximum Range Calculation

Path loss curves, such as the example shown in figure 9, can be very useful in determining the maximum range capability for a particular EM system. If the maximum path loss threshold (to just detect, communicate, or intercept) is known, then the maximum range for that system will be: the range beyond which the path loss is always greater than the threshold. For example, if a 5000 MHz radar has a one-way path loss detection threshold of 160 dB, for a 90 percent probability of detection of a 1 m^2 target for a given false alarm rate, then figure 9 would indicate a maximum detection range of 25 nmi if the radar were at 60 ft and the target at 100 ft. The one-way path loss threshold can always be calculated from equation (4) if the maximum free space range is known for the particular system. Again, for the case of the example, if the system is known to have a maximum free space range of 100 nmi, then equation (4) results in a path loss threshold of 151.8 dB and figure 9 would imply a maximum range (for standard atmospheric conditions) of 21 nmi.

Sometimes, a more convenient form to display the performance capability of an EM system is the vertical coverage diagram, which shows those areas on a height-versus-range plot, where the path loss values are always less than the path loss threshold just described. Figure 10 is an example of such a coverage diagram for a standard atmosphere for the 220 MHz SPS-28 air-search radar, operating at 80 ft above the sea surface and based on a free space detection range of 100 nmi. The shaded area in the diagram represents the area in which the path loss is less than the threshold for detection and, therefore, represents the area where the radar would be expected to detect air targets. The display clearly shows the effects of the interference region with the lobes that extend out to 200 nmi and the deep interference nulls that

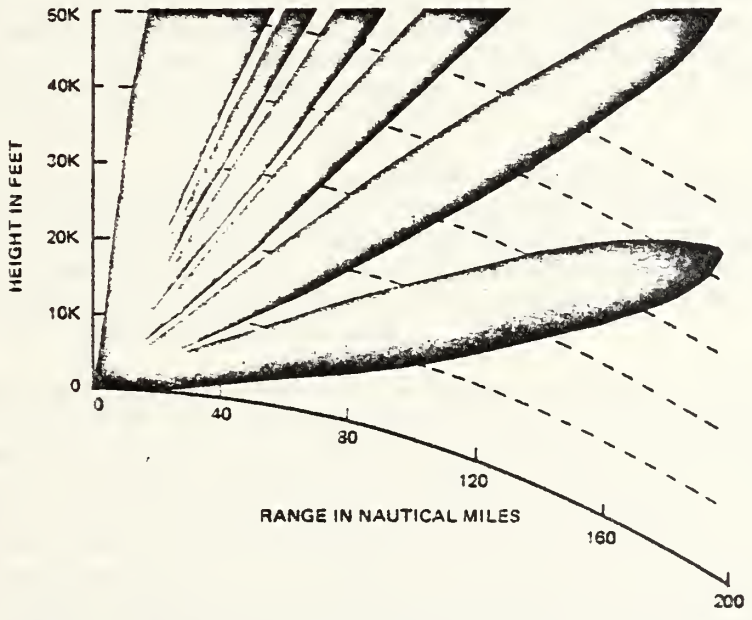

Figure 10. Coverage diagram for the 220 MHz SPS-28 air-search radar at 80 ft for a standard atmosphere and based on a free-space detection range of 100 nmi.

reduce the detection range to within 40 nmi. The lower edge of the bottom lobe, determined by calculations in the diffraction region, is the maximum range for each altitude. The curved-earth display is usually used in the coverage diagrams, because it has been found easy to understand and it simplifies some of the computer routines used to generate the coverage diagrams.

2.3 SURFACE-BASED DUCTS FROM ELEVATED REFRACTIVE LAYERS

Over ocean areas, there often exists a cool moist marine air mass extending vertically, from the ocean surface, to an altitude of up to a few hundred metres. The air mass well above this altitude can be much warmer and drier than the marine air, for a variety of reasons, and it creates a transition region in which the air warms up and dries out rapidly with increasing altitude. The warming and drying of the air causes the modified refractivity to decrease with height, thus forming a trapping layer as illustrated in figure 11. As discussed earlier, if the M-value at the top of the trapping layer is less than the M-value at the ocean surface, a surface-based duct will be formed. To some extent, this kind of duct will trap EM signals at all frequencies of concern, independent of the height of the trapping layer, and will generally give extended radar detection range of surface targets, as illustrated in figure 12.

In addition, surface-based air-search radars can be dramatically affected by surface-based ducts for detection of air targets flying within the duct. Figure 13 shows a coverage diagram for the SPS-28 radar with the same parameters as in figure 10, but in the presence of a 1000 ft high surface-based duct. Note that the detection of air targets flying within the first 1000 ft can be detected at ranges up to 115 nmi which is about 3 times as far as they could have been detected in a standard atmosphere. The amount of range enhancement within the duct is dependent on the radar frequency, with higher frequency radars giving greater detection ranges. Since the SPS-28 uses the lowest Navy radar frequency band, figure 13 represents the minimum enhancement that might be expected in a surface-based duct. Note also, that the lowest interference lobes have been refracted downward, compared to the corresponding lobes shown for a standard atmosphere in figure 10. Such downward refraction is typical in the presence of surface-based ducts.

Surface-based ducts also greatly affect communications and EW systems, with the maximum effects occurring when both the transmitter and receiver are within the duct. Shipboard ESM receivers can particularly benefit from this type of duct, which can result in intercept ranges dramatically greater than those under standard atmospheric conditions. Also, ship-to-ship uhf communications (or ship-to-air for low flying aircraft) can be enhanced to many times the normal communications range.

The rate of occurrence of surface-based ducts created by elevated refractive layers depends on geographic location, season, and time of day. They are usually rare at the extreme northern or southern latitudes (occurring perhaps 1 percent of the time, or less), but can occur up to as much as 20 to 40 percent of the time in some important operational areas such as the southern California off-shore area, the eastern Mediterranean, or the northern Indian Ocean. Also, surface-based ducts tend to occur more often during the warmer months and during daylight hours. On a day-to-day basis surface-based ducts can only be detected by making some measurement of the refractivity of the lower atmosphere at least up to 1 km (3000 ft). These measurements are normally made either using a radiosonde or microwave refractometer. Both of these measurements will be described in section 2.7.1.

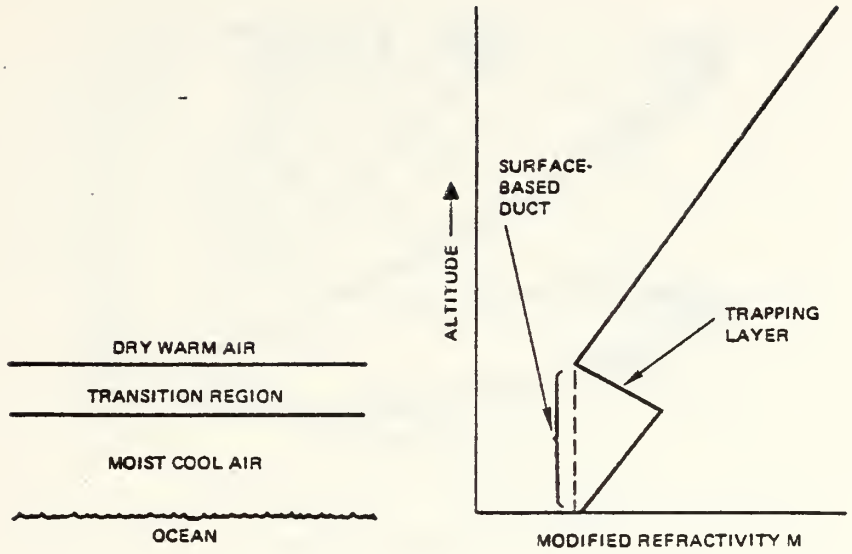

Figure 11. Air masses and transition region responsible for the trapping layer and resulting surface-based duct shown on the right.

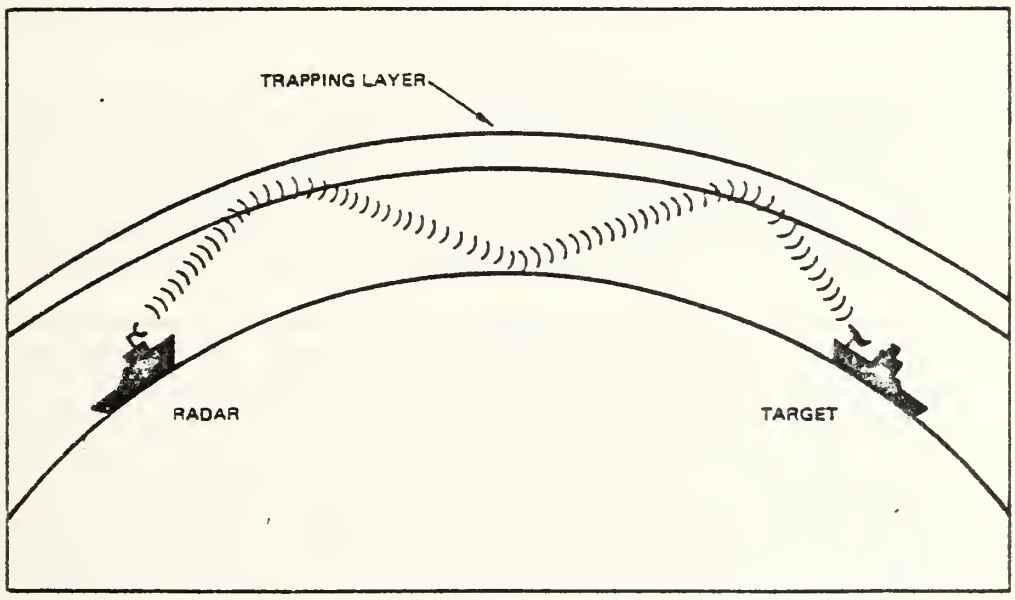

Figure 12. Radar wave path for a surface-based duct created by an elevated trapping layer.

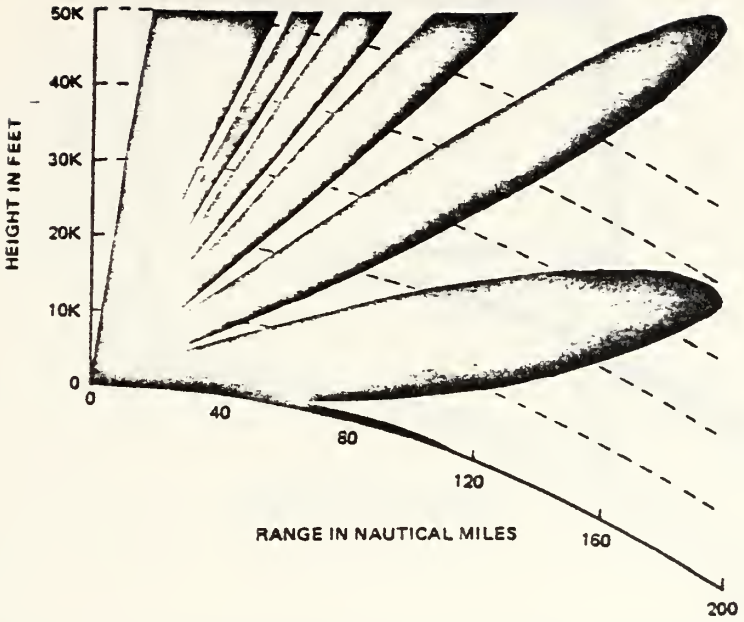

Figure 13. Coverage diagram for the 220 MHz SPS-28 air-search radar at 80 ft for a 1000 ft high surface-based duct and based on a free-space detection range of 100 nmi.

2.4 ELEVATED DUCTS

When the transition region described in the previous section occurs at a higher altitude, than necessary to produce a surface-based duct, then an elevated duct is formed. The N and M unit profiles typical of an elevated duct were previously discussed and illustrated in figure 5. It should be noted that the meteorological process responsible for both surface-based and elevated ducts is identical: namely, the transition between two differing air masses creates a trapping layer. In fact, a surface-based duct can become an elevated duct, and vice-versa, by relatively small changes in the strength or vertical location of the trapping layer.

Although very low elevated ducts can give enhanced performance ranges to surface-based EM systems, the most dramatic effects caused by elevated ducts are for airborne EM systems. An airborne early-warning radar, for example, can utilize elevated ducts to increase its detection range for targets located within the elevated duct if the radar is also in the duct. Figures 14 to 16 illustrate the effect of a strong elevated duct on a typical airborne radar, with a 150 nmi free space detection range, for three radar altitudes. The elevated duct occurs between 15 000 and 17 000 ft and figure 14 shows the enhanced range capability within the duct if the radar is located at 16 000 ft. Notice, however, the large gap in coverage beginning at about 40 nmi and extending outwards above the elevated duct. This gap is often referred to as a "radar hole" and is caused by the trapping of that portion of the wave front within the duct that would normally be in the gap. Actually, the term "radar hole" is not a very good description of the effect because it is possible to detect targets in certain cases within

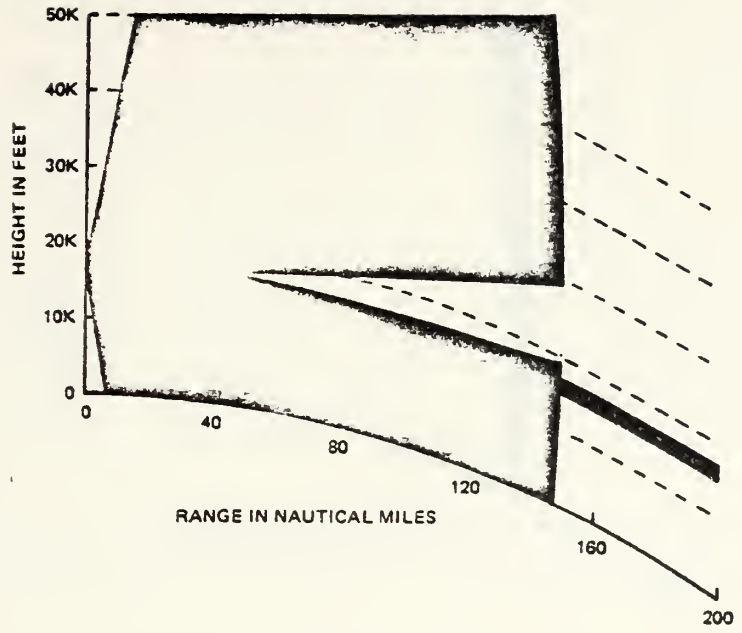

Figure 14. Coverage diagram for typical airborne early-warning radar with 150 nmi free space detection range in the presence of a 15 to 17 kft elevated duct. Radar altitude is 16 kft.

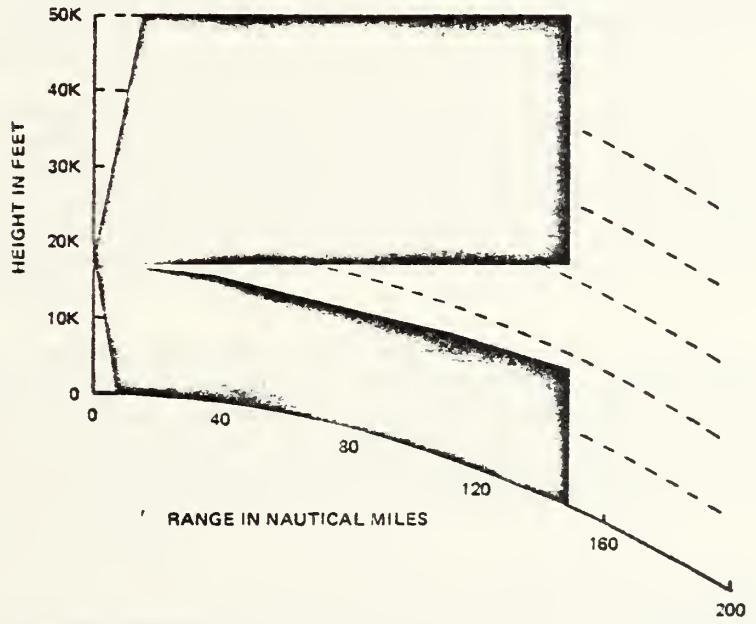

Figure 15. Coverage diagram for typical airborne early-warning radar with 150 nmi free space detection range in the presence of a 15 to 17 kft elevated duct. Radar altitude is 17 kft.

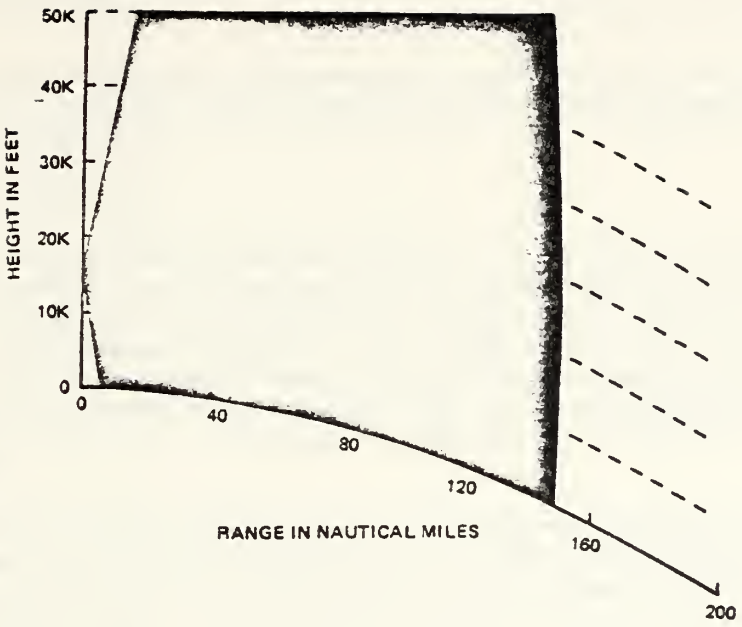

Figure 16. Coverage diagram for typical airborne early-warning radar with 150 nmi free space detection range in the presence of a 15 to 17 kft elevated duct. Radar altitude is 15 kft.

this region, due to energy that escapes or leaks out of the duct or propagates to this region via other paths or mechanisms. Generally, however, the detection of air targets in the gap region is significantly reduced and the term "radar hole" has become widely accepted.

Figure 15 shows the effect of moving the radar up to the very top of the duct to 17 000 ft which results in no enhanced detection capability within the duct, but still creates a large hole in the coverage diagram. If the radar were to be placed at even higher altitudes, then the radar hole would begin at increasing ranges and become smaller until, finally, the hole would begin at a range exceeding the normal maximum detection range and would become inconsequential. In fact, figure 15 shows the worst altitude to place the radar, since the largest hole will result.

Figure 16 shows the effect of placing the radar at the very bottom of the duct, at 15 000 ft, which results in no hole at all. Any radar altitude below an elevated duct will never result in a radar hole and can therefore be the optimum location to minimize the radar hole problem. However, if the elevated duct is low enough, then being below it can cause a reduced horizon problem that can affect overall radar coverage. In the example, the radar is still high enough so that the radar horizon is in excess of the maximum range of the radar, so there is no reduced coverage.

Elevated ducts can affect air-to-air communications and ESM intercept ranges in much the same way as the radar cases described above. The effects are somewhat frequency dependent for all EM systems, with the higher frequencies being the most likely to follow the effects

illustrated by the radar examples. Lower frequencies may not be trapped sufficiently to cause all the effects illustrated.

To properly assess the effects of elevated ducts, a measurement of the refractivity of the atmosphere is needed which is usually accomplished with a radiosonde or microwave refractometer. See section 2.7.1.

2.5 EVAPORATION DUCTS

A very persistent ducting mechanism is created over ocean areas by the rapid decrease of moisture immediately above the ocean surface. For continuity reasons, the air adjacent to the ocean is saturated with water vapor and the relative humidity is thus 100 percent. This high relative humidity decreases rapidly in the first few metres to an ambient value which depends on varying meteorological conditions. The rapid decrease of humidity initially causes the modified refractivity M to decrease with height; but at greater heights, the humidity distribution will cause M to reach a minimum and thereafter increase with height, as illustrated in figure 17.

The height at which M reaches a minimum value is called the evaporation duct height and is a measure of the *strength* of the evaporation duct. The evaporation duct, which extends from the surface up to the duct height, is much thinner and weaker than the surface-based ducts described earlier. As a result, the effect that the evaporation duct will have on EM systems is very dependent on the particular frequency and, to a lesser extent, on the height of the antenna above water. Generally, the evaporation duct will only affect surface-to-surface EM systems, although some effects can occur for relatively low flying aircraft. It must be emphasized that the evaporation duct height is only a measure of the *strength* of the duct and is not a height below which an antenna must be located to give extended ranges. For a given surface-search radar, detection range will generally increase as the duct increases and, for sufficiently large duct heights, surface targets will be detected at ranges significantly beyond the horizon, as illustrated in figure 18. The frequency of occurrence of duct heights sufficiently large to give beyond-the-horizon detection capability to a particular radar varies significantly according to geographic location, season, and time of day. Generally, duct heights will be greater at latitudes nearer the equator, during the summer season, and during daylight hours. For example, duct heights large enough to extend the detection range of the most common surface-search radar, the SPS-10, occur 82 percent of the time in the eastern Mediterranean during summer days, but only 1 percent of the time in the Norwegian Sea during winter nights.

To illustrate these concepts, figure 19 shows the relationship between maximum detection range and evaporation duct height for the SPS-10 surface-search radar. The radar antenna in this case is at 39 metres above the sea surface and a 35 000 square-metre radar cross-section target 10 metres above sea level was assumed, corresponding to a naval warship of destroyer size. The maximum detection range has been calculated, based on a 90 percent probability of detection, a 1×10^{-8} false alarm rate, a steady target, and 5 dB of system loss. Figure 19 shows a detection range of 22 nmi (corresponding closely to the normal radar horizon) for a duct height of zero and increasing detection range for increasing duct heights.

Generally, the evaporation duct is only strong enough to affect EM systems operating above about 3 GHz, although systems with frequencies down to about 1 GHz can benefit

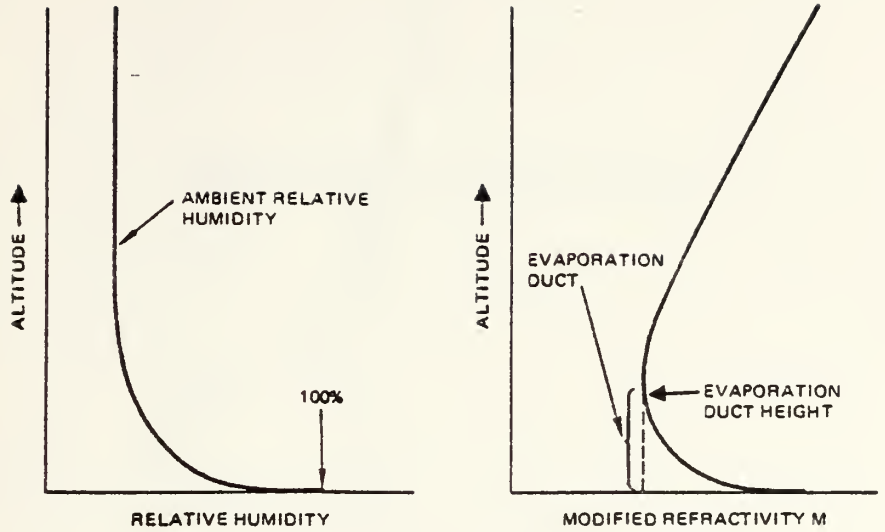

Figure 17. Relative humidity and modified refractivity M versus altitude for an evaporation duct.

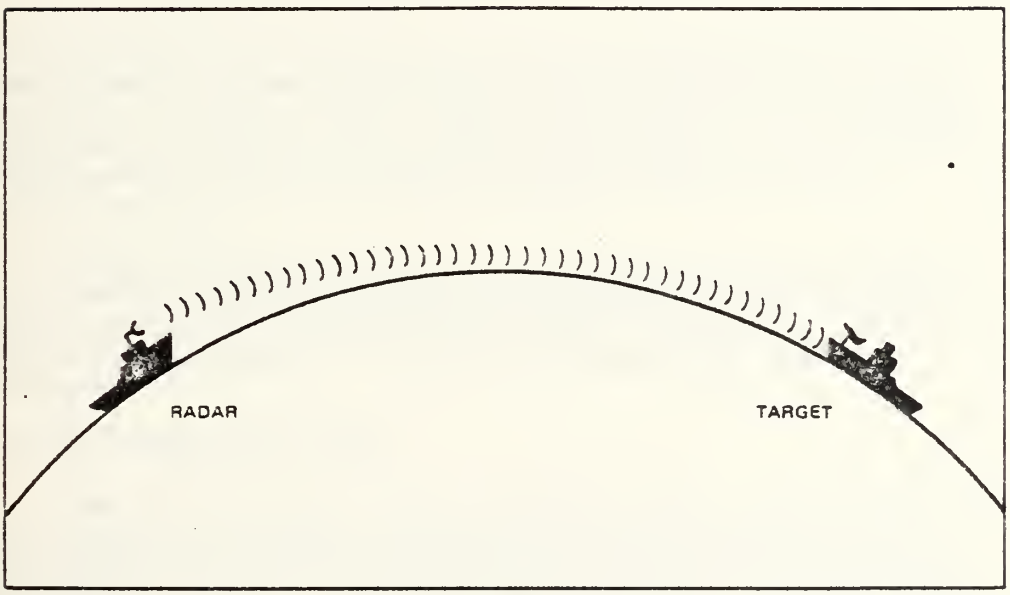

Figure 18. Radar wave path under evaporation ducting conditions resulting in beyond-the-horizon detection.

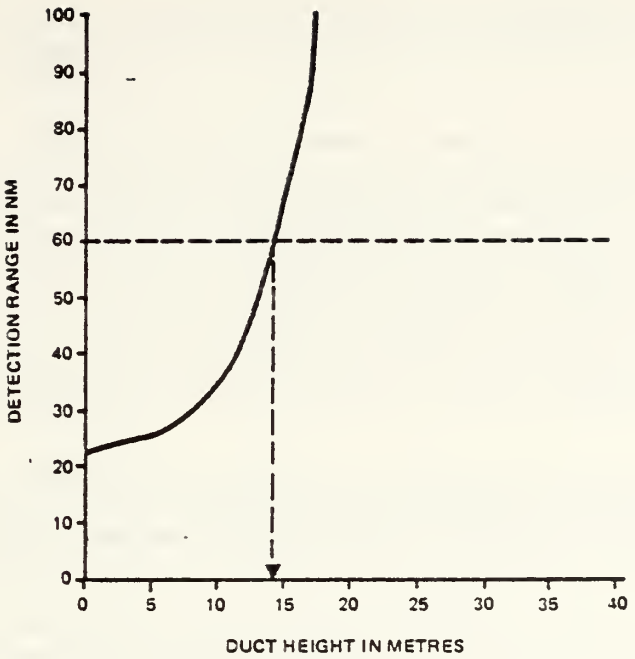

Figure 19. Detection range versus evaporation duct height for the SPS-10 for an antenna height of 39 metres and 90% probability of detection of a destroyer-sized surface target.

from the mechanism on occasion. ESM intercept ranges for surface-to-surface paths can be greatly extended by the evaporation duct and certain communications systems, such as the Multi-Channel Jezebel Relay, could also experience enhanced ranges when both terminals are near the ocean surface. Ship-to-ship uhf communications frequencies are too low to benefit from the evaporation duct, but uhf ranges can be extended by surface-based ducts as explained in section 2.3.

The proper assessment of the evaporation duct can only be performed by making surface meteorological measurements and inferring the duct height from the known meteorological processes occurring at the air/sea interface, as will be briefly described in section 2.7.2. The evaporation duct height *cannot* be measured using a radiosonde or microwave refractometer.

2.6 SEA CLUTTER AND DUCTING

Under certain circumstances, a radar's performance is limited by radar returns from the sea surface known as sea clutter. If the sea clutter return is stronger than a target at the same range, then it will be difficult or impossible to detect the target. Many radars use a Moving Target Indicator (MTI) to enhance the radar's ability to detect fast moving air targets in the presence of sea clutter, by using sophisticated signal processing techniques that depend on the doppler shift of the radar frequency associated with moving targets. MTI is usually sufficient to overcome the sea clutter problem in normal circumstances, but in the presence

of surface-based or evaporation ducts the sea clutter return can be greatly enhanced and overcome the MTI ability to detect the moving target. In addition, the horizontal extent of sea clutter can be greatly extended during ducting conditions and mask targets over much greater ranges than normal.

Figure 20 illustrates how a surface-based duct created by an elevated layer can result in sea-clutter return from a significant range, that can mask air targets at the same range. The strength of the sea-clutter return is very dependent on the strength of the duct and on the roughness of the sea surface which is controlled primarily by the surface wind speed and direction. A surface-based duct, such as that illustrated in figure 20, usually results in several discrete range intervals of high sea clutter because of the typical propagation path in a surface-based duct (fig 12). These discrete intervals are normally independent of azimuth angle, which can give the appearance of sea-clutter rings centered at the radar when viewed on a PPI display. Evaporation ducts, on the other hand, will result in continuous, enhanced sea-clutter return with range.

Airborne radars are also affected by sea clutter and can have their performance severely impaired by enhanced clutter from ducting conditions, particularly for surface-search applications. Often, nearby land clutter, as well as sea clutter, can be significantly enhanced which can cause target masking and general confusion to the radar operator.

The amount of sea-clutter return is very difficult to calculate for ducting conditions and no known algorithms yet exist for programs such as IREPS to take this mechanism into account for radar coverage displays.

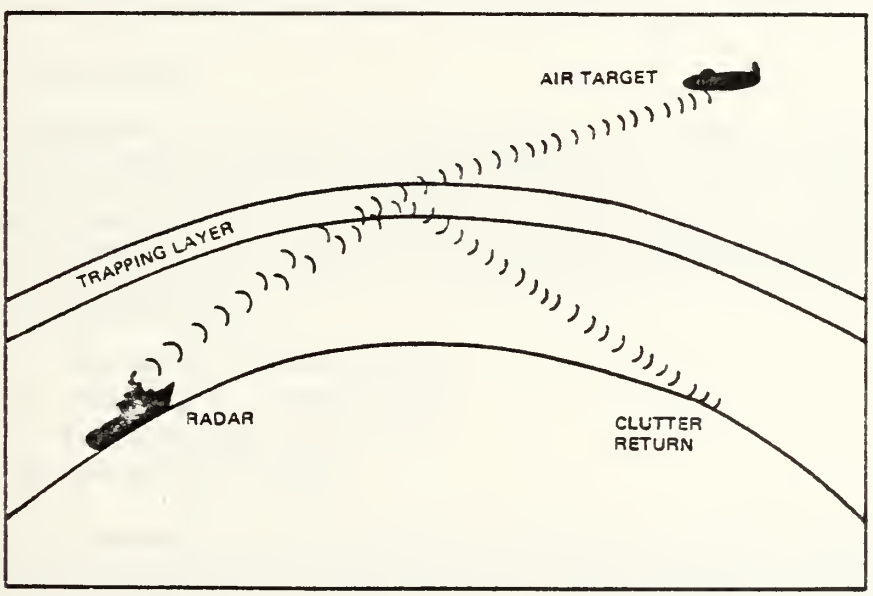

Figure 20. Air-search radar geometry showing possible clutter return from rough sea surface at same range as air target for a surface-based duct.

2.7 METEOROLOGICAL MEASUREMENTS TO ASSESS REFRACTIVE EFFECTS

This section describes measurements that can be taken in-situ to assess refractive effects as they change with the changing environment.

2.7.1 Surface-based and Elevated Ducts

To determine the presence of either a surface-based duct or an elevated duct, measurements of the vertical distribution of the refractivity or of the air temperature and humidity must be made. There are two primary methods by which such measurements are made; namely, the microwave refractometer and the radiosonde.

The AMH-3 refractometer is a device, designed for installation aboard the E-2 aircraft, which directly measures refractivity and records it on a magnetic cassette tape for post-flight processing. The processing includes calculations of modified refractivity M which is plotted as a function of altitude, so that the presence and vertical extent of ducts can be determined as previously discussed. However, at the present time the AMH-3 is not operational in the Navy and refractivity information must be calculated from radiosonde measurements.

The radiosonde is a balloon-borne expendable package that measures temperature, humidity, and pressure as the package ascends through the atmosphere. The measurements are sent via a small radio transmitter to a receiver at the surface and recorded on a moving paper chart. All CVs, LPHs, LHAs and any surface ship with a mobile meteorological team embarked are equipped to operate the equipment and translate the results into refractivity as functions of height. The IREPS program can use inputs, either from the refractometer or the radiosonde, in assessing refractive effects. This will be explained in section 3.4.

2.7.2 Evaporation Ducts

To determine the evaporation duct height at any given time and place, a method has been devised that requires measurements of sea temperature; and at a convenient height above the sea surface, air temperature, humidity, and wind speed. This method is based on the known variation of temperature and humidity near the air/sea interface. It should be noted that the evaporation duct height cannot be determined from normal radiosonde or refractometer data, but must be determined by the method presented in this section. The four required measurements are:

TS: Sea Temperature in degrees Celsius,

TA: Air Temperature in degrees Celsius,

RH: Relative Humidity in percent, and

WS: True Wind Speed in knots.

TS is a measurement of the sea temperature, at the surface, and is best measured with an accurate thermometer and a small bucket which has been lowered into water undisturbed by the ship's wake. Injection water temperature measurements by themselves are generally very inaccurate for the purposes required here and should be avoided if at all possible. It is recognized that obtaining a good sea surface temperature measurement, while underway at reasonable ship speeds, can be very difficult. For ships so equipped, satisfactory measurements

should be attainable through the use of expendable bathythermographs (XBTs). Other equipments that could be used, but which are not normally in ship's allowance, are specially designed "bucket thermometers."

A single measurement of TA and RH is required at any convenient height aboard ship above 6 metres (20 ft) but must be made in a way to minimize any ship-induced effects such as heating. These measurements are best performed with a hand-held psychrometer (such as the ML-450A/UM), pointing the instrument into the wind from the most windward side of the ship.

For the measurement of WS, the ship's anemometer corrected for the ship's course and speed is sufficient. With these required inputs, IREPS can accurately calculate the evaporation duct height and then use the duct height in calculating its effects on the various EM systems.

3.0 OPERATION

3.1 THE IREPS PRODUCTS

After the proper environmental data has been entered into IREPS, as will be explained in detail in section 3.4, there are four basic products that can be requested from IREPS. These four products are:

(1) a propagation conditions summary

(2) a printout (alphanumeric listing) of the environmental data

(3) a coverage diagram

(4) a path loss diagram.

Each product is produced on an 8-1/2 by 11 inch printout consisting of a mixture of alphanumeric labels and graphics displays. There are a number of other displays that IREPS generates on the CRT that are intended to help the operator enter data, select products, and otherwise run the program; but, these cannot be printed out and are not considered IREPS products.

3.1.1 The Propagation Conditions Summary

Figure 21 shows an example of the propagation conditions summary. This product is used to show the existing refractive conditions for the location and date/time of the environmental data set and to give a plain language narrative assessment of what effects may be expected on an EM system-independent basis. The summary shows a refractivity in N-units and a modified refractivity in M-units plot versus altitude. The presence and vertical extent of any ducts are shown by shaded areas on the vertical bar at the right hand side of the product. In this case there is a surface-based duct created by an elevated layer extending up to about 1100 ft. The wind speed and evaporation duct height are listed numerically on this product. Near the bottom of the product are three categories labeled SURFACE-TO-SURFACE, SURFACE-TO-AIR, and AIR-TO-AIR in which occur brief statements concerning the general performance of EM systems in each geometry category. The statements are system independent assessments and are true only in a general sense. For specific systems, one of the other products must be generated in order to obtain a proper assessment of its performance. The bottom line of the summary lists the surface refractivity and the setting for the SPS-48 height-finder radar to properly account for refractive effects in its calculations of elevation angle and height.

3.1.2 The Environmental Data List

Figure 22 is an example of the environmental data list product that is used primarily for checking numeric values of data entries that provide numeric values of dew point depression, altitude, N units, N unit gradient, M units, and a description of the refractive condition. Also, this product can be used to archive environmental data sets for future use, since all required input values are listed numerically. In addition, the last line of this product is the same as that of the summary which displays surface refractivity and the proper setting for the SPS-48.

**** PROPAGATION CONDITIONS SUMMARY ****

LOCATION: 31 56N 118 36W
DATE/TIME: 17 JUN 0045Z

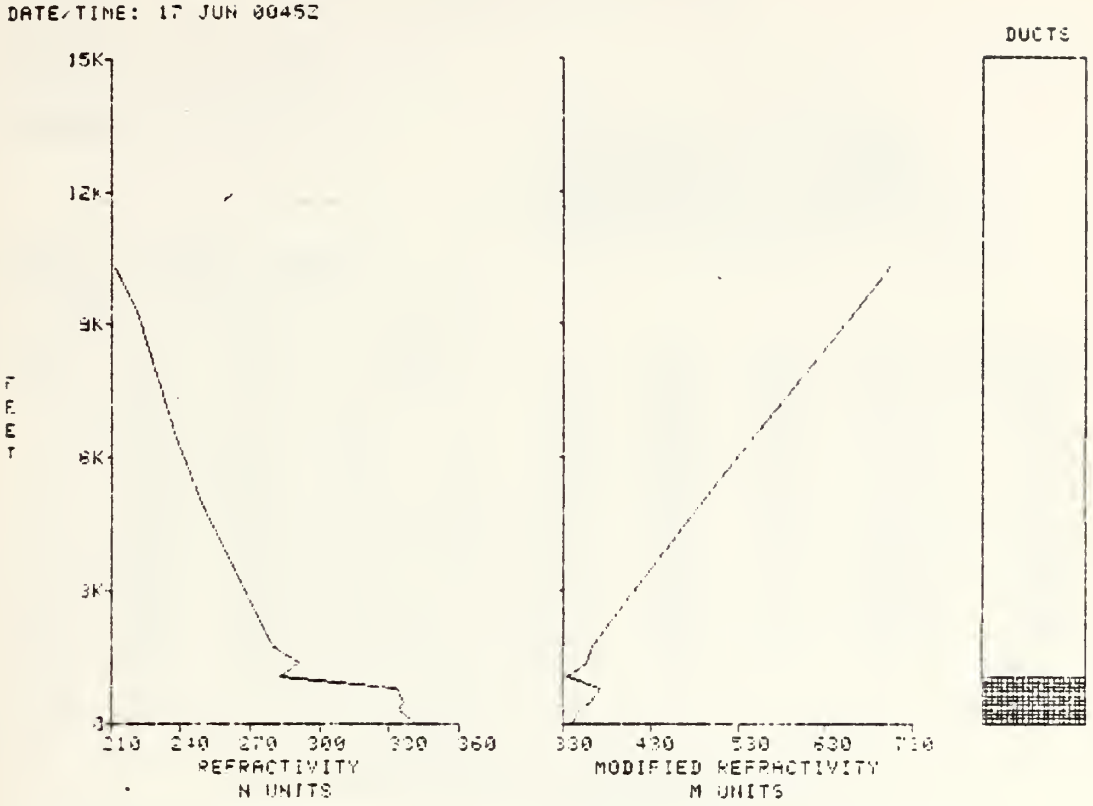

WIND SPEED 12.0 KNOTS

EVAPORATION DUCT HEIGHT 28.0 FEET
EVAPORATION DUCT HEIGHT 8.5 METRES

SURFACE-TO-SURFACE
EXTENDED RANGES AT ALL FREQUENCIES

SURFACE-TO-AIR
EXTENDED RANGES FOR ALTITUDES UP TO 1,072 FEET
POSSIBLE HOLES FOR ALTITUDES ABOVE 1,072 FEET

AIR-TO-AIR
EXTENDED RANGES FOR ALTITUDES UP TO 1,072 FEET
POSSIBLE HOLES FOR ALTITUDES ABOVE 1,072 FEET

SURFACE REFRACTIVITY: 341 ---SET SPS-48 TO 344

Figure 21. Propagation conditions summary product.

```
                    **** ENVIRONMENTAL DATA LIST ****

LOCATION: 31 50N  118 36W
DATE/TIME: 17 JUN 0045Z

WIND SPEED  12.0  KNOTS                  EVAPORATION DUCT PARAMETERS:
                                         SEA TEMPERATURE  18.2 DEGREES C
                                         AIR TEMPERATURE  15.1 DEGREES C
                                         RELATIVE HUMIDITY 89 PERCENT
                                         EVAPORATION DUCT HEIGHT 28.0 FEET
                                         EVAPORATION DUCT HEIGHT 8.5 METRES
SURFACE PRESSURE = 1008.0 mB
RADIOSONDE LAUNCH HEIGHT = 60.0  FEET

       PRESS     TEMP     RH    DEW PT
LEVEL   (mB)      (C)     (%)   DEP(C)     FEET      N UNITS   N/Kft   M UNITS   CONDITION
  0     ------    ----    ----  ----         0.0     340.7    -12.0     340.7     NORMAL
  1   1,008.0     15.1    89.0    1.8       60.0     340.0    -28.2     342.9     SUPER
  2   1,000.0     14.2    87.0    2.1      281.6     333.8     15.6     347.2       SUB
  3     993.0     13.9    95.0     .8      476.6     336.3    -10.9     359.6     NORMAL
  4     982.0     13.3    97.0     .5      785.3     333.4   -176.4     371.0       TRAP
  5     972.0     20.4    25.0   20.8    1,071.8     282.9     27.2     334.2       SUB
  6     962.0     21.5    34.0   16.6    1,364.9     290.9    -28.9     356.2     SUPER
  7     949.0     21.5    27.0   19.9    1,751.3     279.7     -9.4     363.5     NORMAL
  8     862.6     20.6    25.0   20.8    4,477.3     254.0     -9.5     468.2     NORMAL
  9     850.0     19.7    25.0   20.7    4,873.5     250.2     -7.6     483.4     NORMAL
 10     807.0     20.0    25.0   20.7    6,339.1     239.0     -6.0     542.3     NORMAL
 11     726.2     14.5    34.0   15.8    9,299.4     221.2     -8.9     666.1     NORMAL
 12     700.0     11.8    34.0   15.5   10,305.6     212.2     ------   705.3     ------

SURFACE REFRACTIVITY: 341 ---SET SPS-48 TO 344
```

Figure 22. Environmental data list product.

3.1.3 The Coverage Display

Figure 23 is an example of an IREPS coverage display product that shows the area of coverage on a curved-earth range-versus-height plot. The shaded area in the plot corresponds to the area of detection or communication which, in this example, is based on a 50 nmi free space detection range for a 1300 MHz SPS-12 air-search radar operating at 100 ft above the sea surface. In other words, if this radar could detect a certain target at 50 nmi in free space, then it will actually detect the same target anywhere within the shaded area. In addition to the basic coverage display plot, this product also includes the location and date/time labels for the refractivity conditions upon which it is based and labels to describe the type of system and detection definition, plus a numeric listing of the free space range, the frequency, and the transmitter or radar antenna height.

The coverage display has a number of uses in assessing both radar and communications coverage. It is useful to many squadrons in planning flight profiles and to CIC or TSC shipboard personnel in planning and controlling airborne platform locations. A more complete list of tactical uses of this product will be presented in section 3.3.

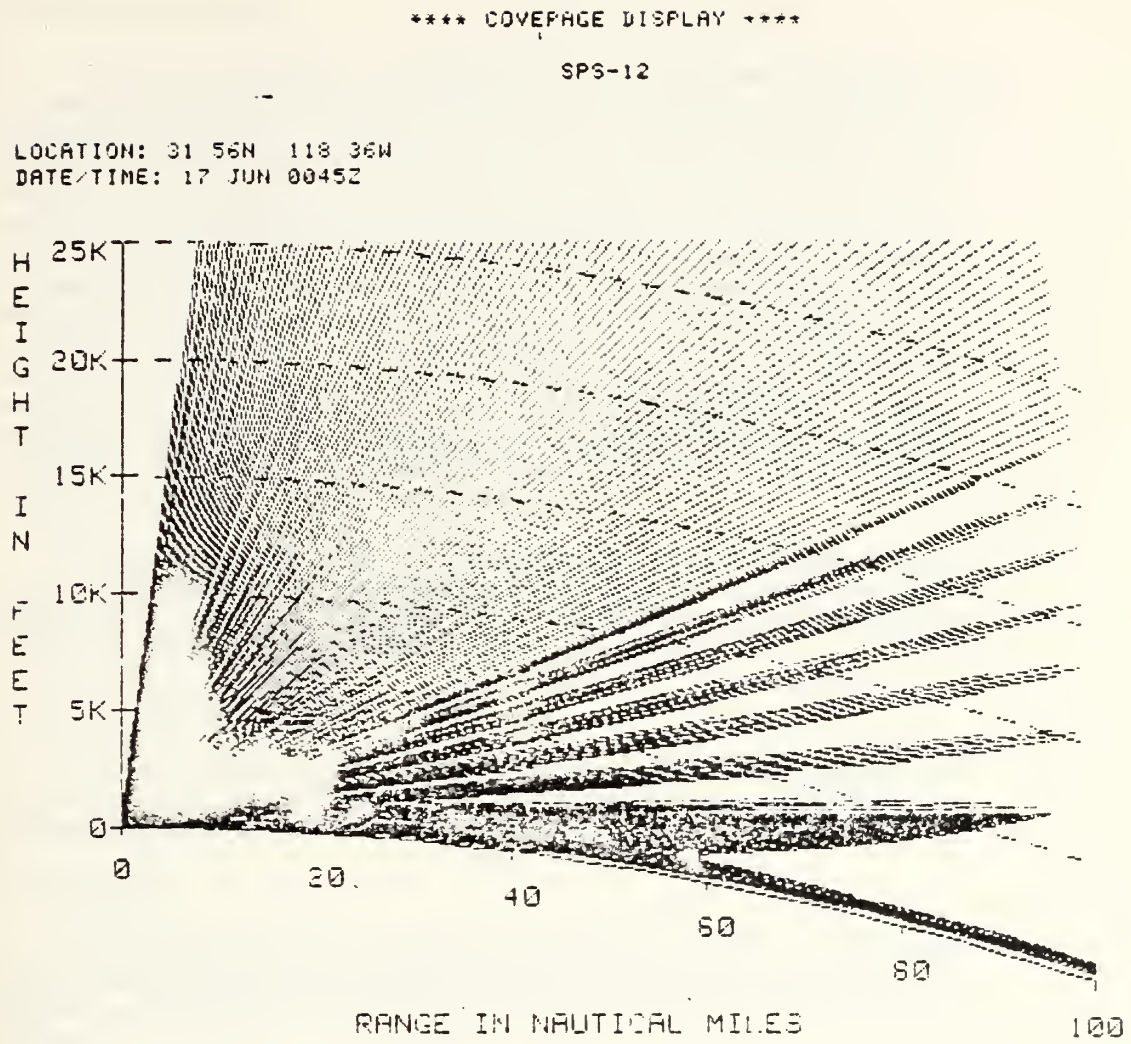

Figure 23. Coverage display product.

3.1.4 The-Path-Loss Display

Figure 24 is an example of path loss display product that shows one-way path loss in dB versus range. The dashed line in the display represents the threshold for detection, communication, or intercept. In the example, it is based on a 50 percent probability of detection of a destroyer-sized surface target, with a false alarm rate of 1×10^{-8} for the 5600 MHz SPS-10 surface-search radar. In the example, the radar is located at 160 ft and the target is located at 50 ft above the ocean surface. The display shows path loss to be less than the threshold, out to 100 nmi in the example; hence, detection would be expected at all ranges up to 100 nmi. The example is for the refractive conditions of figure 21 which are characterized by a strong surface-based duct. If there were no duct, then the path loss in figure 24 would have crossed the detection threshold at about 25 nmi. In addition to the basic path loss plot, this product also includes the labels for location and date/time for the applicable refractivity conditions, labels to describe the system and definition of detection, numeric values for the free space range, frequency, transmitter/radar height, and receiver/target height. The path loss at the dashed line threshold is the one-way free space path loss from equation (4) based on the free space range listed.

The path loss display is very useful in assessing surface-search radar ranges, communication ranges, ESM intercept ranges, and many other applications when both the transmitter and receiver (or radar and target) heights can be specified. A more complete discussion of tactical uses of the loss display will be presented in section 3.3.

3.2 LIMITATIONS OF THE IREPS MODELS

There are a number of limitations in the IREPS models and resulting displays that the user needs to be aware of. The IREPS models and software are constantly undergoing revisions and many of the limitations discussed here will be overcome in the near future.

3.2.1 Frequency

The frequency range for which the models have been developed is from 100 MHz to 20 GHz. Any use of the IREPS program for frequencies outside these bounds is improper and erroneous assessments are likely to result. The models specifically do not apply to any hf system.

3.2.2 Clutter

The models do not include any effects produced by sea or land clutter in the calculation of radar detection ranges. This shortcoming may be of importance for air-search radars in the detection of targets flying above surface-based or strong evaporation ducts, but it is not expected to affect significantly the predicted enhanced detection ranges within a duct. Specifically, for surface-based ducts, the actual detection capability at some ranges may be reduced for air targets flying above the duct.

3.2.3 Horizontal Homogeneity

The IREPS program does not allow for horizontal changes in the refractivity structure. This restriction is not believed to be a serious one, since there exists scientific evidence

**** LOSS DISPLAY ****

SPS-10/DD

LOCATION: 31 56N 118 36W
DATE/TIME: 17 JUN 0045Z

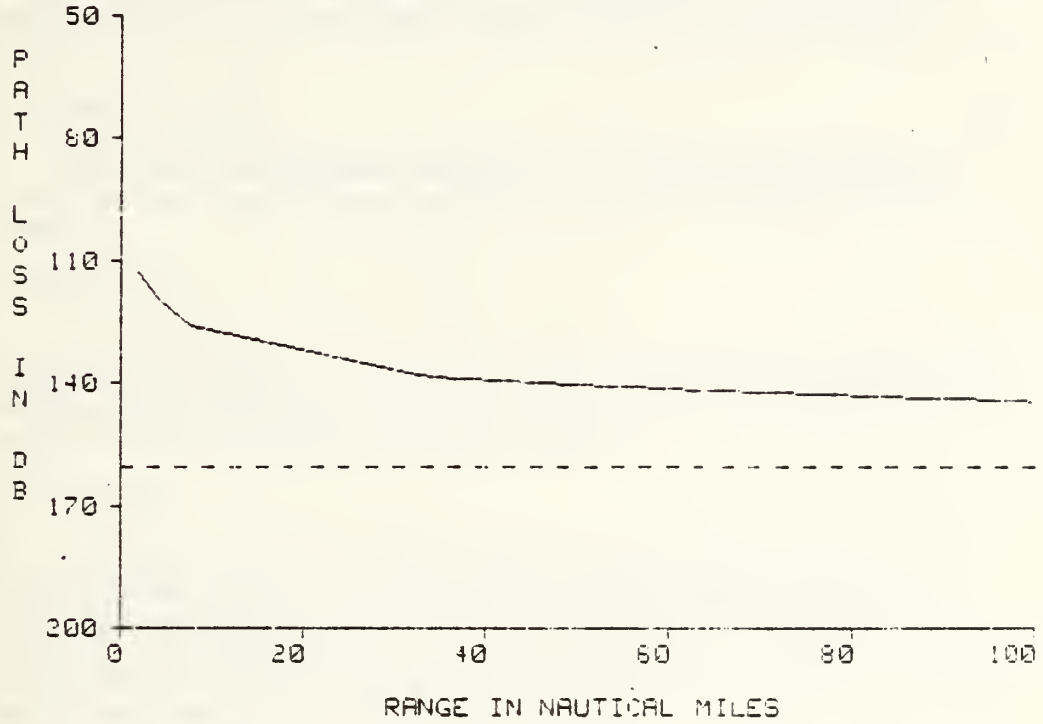

SURFACE-SEARCH RADAR
FOR 50 % POD OF DESTROYER-SIZED SURFACE TARGET

DASHED LINE INDICATES DETECTION, COMMUNICATION, OR INTERCEPT THRESHOLD

FREE SPACE RANGE: 248.4 NAUTICAL MILES
FREQUENCY: 5600 MHZ
TRANSMITTER RADAR HEIGHT: 150 FEET
RECEIVER/TARGET HEIGHT: 50 FEET

Figure 24. Loss product.

that the assumption of a horizontally homogeneous atmosphere is valid about 85 percent of the time for the purpose of making refractive effects assessments. The IREPS operator, and also the users of the IREPS products, should be aware of the changing state of the atmosphere and try to acquire and use refractivity measurements that are appropriate to the planned time and place of the pertinent operations.

3.2.4 Antenna Heights

The model that calculates the coverage display for surface-based systems is valid only for antenna heights between 3 and 250 ft. This should not be a restriction to any normal application for ship based systems, including submarines operating at periscope depth.

3.2.5 Interference Effects

The airborne coverage display model does not include sea-reflected interference effects which could cause both reduced and enhanced coverage for low-flying radar or target aircraft.

3.2.6 Polarization

The polarization of all the EM systems is assumed to be horizontal. Almost all radar systems are in fact horizontally polarized, so this limitation should be inconsequential to the radar case. However, some communications systems do employ vertical polarization and a small miscalculation in communication range could result.

3.2.7 Absorption

There is no account made of absorption from oxygen, water vapor, fog, rain, snow, or other particulate matter in the atmosphere. Most of these absorption effects are very minor over the valid frequency range of the models and will not affect the predicted ranges. For very heavy precipitation there may be a noticeable effect; but, even if the precipitation models existed, it would be difficult or impossible to obtain the required precipitation rates and horizontal extent from which calculations could be made.

3.2.8 Path Loss Plot Restrictions

The path loss plot does not include a model to account for propagation in an elevated duct. Also, the path loss plot does not include the interference nulls, but only gives a value in the interference region corresponding to the maximum signal (least loss).

3.3 SOME TACTICAL USES OF THE IREPS PRODUCTS

This section presents some of the tactical uses for the IREPS products as identified through actual fleet experiences. The section is not intended to be a complete list of uses since it is anticipated that many additional users of the products will be discovered as the Interim IREPS becomes generally available on the carriers.

3.3.1 Aircraft Penetration Profile Determination

The standard procedure, for attack and reconnaissance aircraft, in penetrating an enemy target's defenses is to fly as low as possible to remain "beneath the radar coverage." This is valid during non-ducting conditions: however, surface-based ducting conditions often give the enemy a greater detection range capability for targets flying within the duct than with a target at high altitude. Knowledge of the existence and height of a surface-based duct would enable the strike group or aircraft commander to select the optimum altitude for penetration. This would be just above the top of the duct, where an absence of sufficient enemy radar energy exists for detection of targets. The coverage display geared to the adversary's air-search radar is the appropriate IREPS product to use in determining the optimum flight profile. For example, the best profile to avoid detection by the SPS-12, shown in figure 23, would be above the surface-based duct at an altitude of about 1500 ft. In this case, it would also be possible to avoid detection by flying down one of the interference nulls, but the changing height-versus-range profile would be more difficult to fly and if the aircraft were off course or the null pattern changed somewhat, detection would occur. At any rate, the worst place to fly would be at a few hundred ft above the sea, since detection here would occur at a greater range than at any other height.

3.3.2 Disposition of Forces

A knowledge of the presence or absence of surface-based ducting conditions gives the OTC a greater flexibility in deciding the disposition of his units. Fox example, if an OTC wishes to utilize a widely dispersed formation, yet maintain communications between units, he may do so under surface ducting conditions without the necessity of a middleman relay in the uhf communications link. The absence of ducting conditions dictates the use of a middleman. Knowledge of the presence of surface-based ducting also provides the possibility of uhf backup to over-the-horizon hf communications, ship-to-ship and ship-to-shore (e.g., CV to divert field). The path loss display, geared to uhf communications, is the proper IREPS product to use in assessing changes in refractive effects for such surface-to-surface applications.

3.3.3 ECM Aircraft Positioning

In a manner similar to that described in section 3.3.1, an ECM aircraft can adjust its position to maximize the effectiveness of its jammers by using the appropriate coverage display. Also, the range at which the jammers are effective can be extended considerably in the presence of ducting, which can give the ECM aircraft a much better stand-off capability and possibly allow jamming of more widely-spaced threats.

3.3.4 AEW Aircraft Stationing

By using the proper coverage displays, the optimum altitude for AEW aircraft can be determined, which will minimize the effects of radar holes created by elevated ducts. Figures 14 through 16 illustrated the various effects of stationing a typical AEW aircraft within, above, and below an elevated duct. Experience with these displays, for elevated ducts, shows that radar holes are minimized by flying as high above the duct as possible, or by flying anywhere below the duct.

3.3.5 EMCON Conditions

Emission control procedures are a primary tactical application of IREPS products. A knowledge of the existence of a strong surface-based duct is a warning that electromagnetic radiation will be trapped and result in enhanced signals. These can be intercepted at vastly greater ranges (hundreds of miles) than they can under normal conditions. Under ducting conditions, it would be prudent to weigh the benefits of the greatly increased radar search range against the much greater increase in the range a potential enemy gains for detection of the radiation. Even low power radiation sources, such as flight deck communications (Mickey Mouse) systems, have been intercepted at ranges greater than 200 nmi from the CV during ducting conditions.

Knowledge of the existence of ducting conditions enables a commander to maintain silence and detect an unsuspecting enemy hundreds of miles over the radar horizon through EW. Figure 21 showed the IREPS propagation conditions summary which would be most useful in determining EMCON conditions. In the case shown in figure 21, a strong surface-based duct exists to a height of about 1100 ft, causing greatly extended ranges at all frequencies. Under these conditions, the more prudent course of action may be to remain silent.

3.3.6 ASW Tactics

A direct tactical application of the knowledge of the presence of surface-based ducting conditions to communications procedures is found in the use of the Multi-Channel Jezebel Relay system (MCJR). An ASW helicopter engaged in-dipping sonar operations over the line of sight horizon may relay to the ship while maintaining his sonar dip. This is especially important if he gains contact with a submarine and must both relay and maintain contact. If ducting conditions are present, the ASW helicopter knows that he can maintain both ASW surveillance and communications far beyond the normal radio horizon. If no surface-based duct exists, he must raise his sonar and increase altitude until he is above the horizon. In this case, a coverage display geared specifically to the MCJR would be used in assessing communications capability.

3.3.7 Uhf Communications

A coverage display for surface-to-air uhf communications can show the regions in space where communications are possible, considering the effects of the interference region and possible ducting. Independent of an aircraft's mission, it may be able to communicate to the ship by changing its altitude only slightly and exploiting the existing propagation effects. In this case it may even be advisable that the pilot have an IREPS hard copy of the appropriate uhf communications coverage display.

3.3.8 Hardware Performance Assessment

Knowledge of surface-based ducting provides for hardware performance assessment by sea going units. This phenomenon can explain detection of targets over the radar horizon on a given day and preclude unnecessary maintenance calls when similar ranges are not present during non-ducting conditions. False or "ghost" targets may also be a result of ducting conditions and are not always indicative of hardware problems. Coverage diagrams may also be used to assess the performance of the various radars aboard a given unit, by providing a standard for optimum performance under non-ducting conditions and explain anomalies such as extended ranges and "radar holes" under ducting conditions.

LIST OF REFERENCES

1. Skolnik, M. I., Introduction to Radar Systems, 2nd Edition, p. 224, McGraw-Hill Book Company, Inc., New York, 1980.

2. Naval Research Laboratory Report 6930, A Guide To Basic Pulse-Radar Maximum-Radar Calculation. Part 1 - Equations, Definitions, and Aids To Calculation, by L. V. Blake, p. 51, 23 December 1969.

3. Op. Cit., Blake, p. 57.

4. Op. Cit., Blake, p. 53.

5. Naval Ocean Systems Center Technical Report (Preliminary Copy), Propagation Models for IREPS Revision 2.0, by C. P. Hattan, p. 8, 11 February 1982.

6. Op. Cit., Skolnik, p. 449.

7. Op. Cit., Skolnik, p. 445.

8. Op. Cit., Skolnik, p. 451.

9. Naval Ocean Systems Center Draft, IREPS Revision 2.0 User's Manual, by H. V. Hitney, et al., p. 51, September 1981.

10. Op. Cit., Blake,

11. Op. Cit., Skolnik, p. 227.

12. Op. Cit., Blake, p. 70-85.

13. Op. Cit., Skolnik, p. 56-62.

14. Op. Cit., Hattan, p. 8.

15. Op. Cit., Skolnik, p. 450.

16. Op. Cit., Blake, p. 86.

INITIAL DISTRIBUTION LIST

		No. Copies
1.	Defense Technical Information Center Cameron Station Alexandria, Virginia 22314	2
2.	Library, Code 0142 Naval Postgraduate School Monterey, California 93940	2
3.	Superintendent Attn: Chairman, Electronic Warfare Academic Group, Code 73 Naval Postgraduate School Monterey, California 93940	1
4.	Professor Gordon E. Schacher, Code 61Sq Department of Physics and Chemistry Naval Postgraduate School Monterey, California 93940	2
5.	AFEWC/SAT (Captain Thomas White) San Antonio, Texas 78243	1
6.	Dr. Lonnie A. Wilson, Code 62Wi Department of Electrical Engineering Naval Postgraduate School Monterey, California 93940	1
7.	Professor Kenneth L. Davidson, Code 63Ds Department of Meteorology Naval Postgraduate School Monterey, California 93940	1
8.	Professor Jeff Knorr, Code 62Ko Department of Electrical Engineering Naval Postgraduate School Monterey, California 93940	1
9.	Naval Ocean System Center Attn: H.V. Hitney, Code 5325 San Diego, California 92152	1
10.	Headquarters SAC SAC/XOBD Offutt AFB, Nebraska 68113	1

11. Headquarters SAC — 1
SAC/XOO
Offutt AFB, Nebraska 68113

12. Headquarters SAC — 1
SAC/XOBB
Offutt AFB, Nebraska 68113

13. Headquarters SAC — 1
SAC/DOO
Offutt AFB, Nebraska 68113

14. Headquarters SAC — 1
SAC/XOO
Offutt AFB, Nebraska 68113

15. Headquarters SAC — 1
SAC/DOTT
Offutt AFB, Nebraska 68113

16. Capt. Joseph Ford — 1
Code 370
Naval Air System Command
Washington, D.C. 20360

17. Dr. Paul Twitchell — 1
Code 370C
Naval Air Systems Command
Washington, D.C. 20360

18. Mr. San Brand — 1
Naval Environmental Prediction
Research Facility
Monterey, California 93940

19. Capt. Ronald Hughes, Commander — 1
Naval Oceanography Command
NSTL Station, MS 39529

20. Lcdr R. Huff — 1
Code 9220
Naval Oceanographic Office
NSTL Station
Bay St. Louis, MS 39529

21. Mr. Paul Banas — 1
Code 9220
Naval Oceanographic
NSTL Station
Bay St. Louis, MS 39522

22. The Johns Hopkins University 1
Attn: Mr. Dan Henderson
Applied Physics Laboratory
Laurel, Maryland 20810

23. Mr. Brook C. Collier 1
Code 1151
Pacific Missile Test Center
Point Mugu, California 93042

24. Lcdr Jim Griffin 1
VAQ-133
FPO San Francisco, CA 96601

25. Lt. Henry Schrader 1
TAWC/Det 3
Mountain Home AFB, Idaho 83648
Mail Stop 41

26. AFIT/CIRF 1
Wright-Patterson AFB, OH 45433

199640

Thesis
W55535 White
c.1 Positioning of
jamming aircraft
using the integrated
refractive effects
prediction system.